Simplification of CAD Geometries to perform CEM Simulations

Farrukh Bashir

Department of Mechanical Engineering

Blekinge Institute of Technology

Karlskrona, Sweden

2021

Abstract

The purpose of this study is to investigate small features in CAD geometries which have high influence on computational time and memory consumption during electromagnetic simulations using CAE software**.** Computational Electromagnetics (CEM) simulations of complex CAD geometries like passenger cars crash often simulations remain incomplete due to a lot of irrelevant details. The key to eliminating the limitations enumerated above is to remove irrelevant details in CAD geometries within the acceptable margin of accuracy. The maximum 5% percentage of error in accuracy during Computational Electromagnetics (CEM) simulations is compromised. CAD geometry is transferred into CAE geometry. The modification of geometry is done by removing irrelevant details to get optimal mesh and improve the computational time and memory consumption during simulations with ANSA and HYPERMESH software at their best potential. At the end, electromagnetic simulations are done on original and simplified CAD models in CST and in COMSOL. Only magnetic flux density distribution across the modified and unmodified CAD model by cut points 3D on different coordinate positions is analysed. The results are compared with quality of mesh in terms of accuracy and reduction in computational time and memory. The features in CAD geometries are identified, these features can be removed and computational time and memory consumption reduced with minimum loss of accuracy during simulation.

Keywords: CAD, CAE, Defeaturing, Modification, Blending Features, FEA, CEM.

Acknowledgements

This thesis is carried out at the Volvo Cars Corporation Gothenburg Sweden, under the supervision of Leif Kindberg, Anders Bergqvist and PhD Oskar Talcoth. It was initiated in June, 2015 and finished in June, 2016.

I would like to express my sincere appreciation to Volvo Cars for giving me opportunity in research and development of product and all the support I have obtained.

I would like to thank Anders Bergqvist, who provided all support related to management during thesis work at Volvo Cars. I would like to thank PhD Oskar Talcoth for his supervision and professional engagement throughout the thesis work.

I would like to thank my supervisor at Blekinge Institute of Technology, Ansel Berghuvud who has provided feedback to improve the project.

Farrukh Bashir

Table of Contents

Figures

Tables

Abbreviations

ANSA	ANSA Pre-processor
B-rep	Boundary representation
CAD	Computer Aided Design
CAE	Computer Aided Engineering
CST	Computer Simulation Technology
CEM	Computational Electromagnetics
FEA	Finite Element Analysis
HYPERMESH	HYPERMESH Pre-processor
Volvo Cars	Volvo Cars Corporation

1 Introduction

1.1 Background

The analysis and design of electromagnetic structures was done by experiments before digital computers came in the market. Digital computers influenced every one including industries and individuals. Today, every industry is performing simulation on computers for improvement of design at very early stage. Simulation saves time, reduces cost and strengthens the competitiveness of companies. It has become the most important part in research and product development in recent years. The level of details in passenger car makes it very complex for computational electromagnetics (CEM). The complexity of car model increases the computational time and memory during CEM analysis. The electromagnetics simulation does not complete in complex car model due to excessive number of elements by application of finite element method. It stops after half simulation is done or gives errors. Sometime it takes too much time to complete one electromagnetics simulation. This causes waste of time and frustration for simulator because he has to perform simulations again and again on whole car body. If model is simplified, it takes less time for simulation; the detailed analysis can then be performed on model to get accurate and desired results.

1.2 Aim and Purpose

The main scope of the thesis is to investigate how to best adapt CAD models of passenger cars for electromagnetic simulations. Often, a CAD model of an entire car is too complex to be used directly in an electromagnetic simulation with reasonable time and memory consumption. Therefore, models need to be simplified, where details that have negligible effect on the electromagnetic behaviour are removed, or modelled differently. A desirable outcome of the thesis is an efficient workflow for model adaptation, using professional CAD software. Determine the effects on accuracy of various simplifications, and find a good trade-off between accuracy on the one hand, and time and memory consumption on the other. An investigation to give more insight into these issues is also part of the thesis work.

1.3 Limitations

The thesis is composed of two parts. Firstly, finite element model with suitable mesh is prepared, while secondly electromagnetic simulations are applied on prepared model. The model preparation includes, which kind of details should be removed and mesh comparison. The mesh comparison is done from very coarse mesh to very refine mesh. The main focus is to find suitable density of mesh by compromising with accuracy. HYPERMESH and ANSA are proprietary software used to prepare the finite element meshed model. CST and COMSOL are used to simulate the finite element meshed model for electromagnetic analysis. CST is used by thesis supervisor Oskar Talcoth. There are constraints in research, in terms of computer capability, used for simulation and software capabilities.

1.4 Research Question

The thesis will result in answering following research question.

What kind of details can be removed from CAD geometry for simplification of CAD model during CEM, with acceptable loss of accuracy?

1.5 Thesis Outline

Chapter two in report represent capability of CAE softwares relevant in this thesis. Chapter three explains theory of electromagnetics and how this theory has been used in this study. Chapter four give overview of process to build CAD model in ANSA. Chapter five presents result with different comparison to get simple CAD geometry with reduce computational time and memory consumption with acceptable loss of accuracy.

1.6 Methodology

These stages interact with other in whole process. The CAD model simplification and analysis preforms with a lot of iterations till we get the desired results.

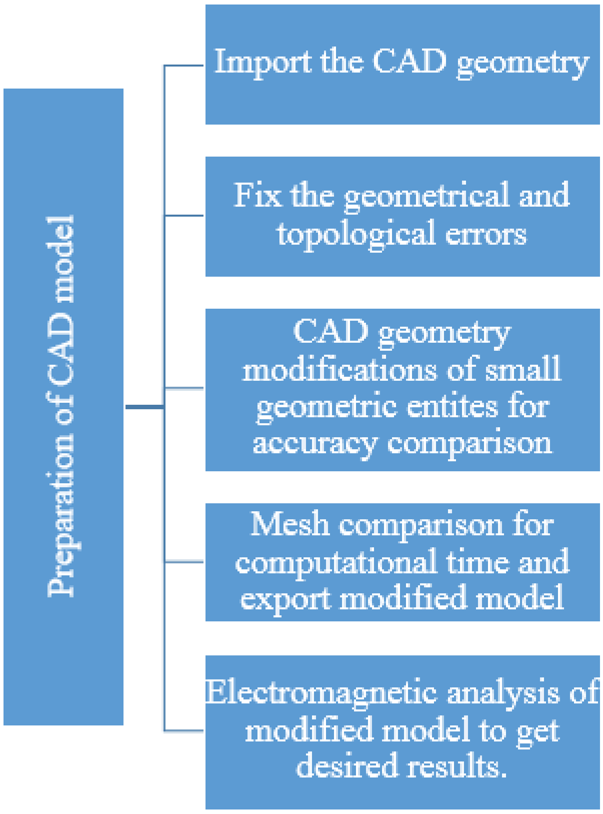

Figure 1-1. Method to follow of CAD model for electromagnetic analysis in this thesis.

1.7 Literature Review

First paragraph of literature review is about preparation of finite element model for optimal mesh generation to reduce time and memory cost for analysis. CAD model has complex geometry with very small details. The optimal mesh need simplified and smooth CAD model. The geometrical and topological errors also affect the mesh model. The all kind of geometrical details are removed from the CAD model to make it suitable for mesh generation with different techniques and methods. Second paragraph is about the electromagnetic analysis on CAD model. The electromagnetic analysis is performed on cable harness of car to get more simplified cable wiring harness. The CAD model of car is compared from complex model to simple model to reduce the computational time and memory in terms of accuracy. The electromagnetic analysis is performed with different techniques and methods. The simplified CAD models of car are used to perform electromagnetic analysis.

The literature review in both paragraphs explores the simplification and electromagnetic analysis of the CAD model. However, the effect of each feature of car CAD model on the accuracy is missing in this literature. We want to investigate particularly small features in CAD models which have high influence on computational time and memory consumption. If these features have small effect on accuracy during electromagnetic analysis, then we will remove them from CAD models. The main focus is to investigate in terms of accuracy all those small entities, which have effect in dense mesh and cause increment in computational time.

The study done by C. Li et al.[1], gives complete overview of the preparation of CAD model for FEA. In this work, little information is given about important aspects like CAD file transfer into CAE system, Defeaturing and mesh generation. In study done by David Krutilek and Zbynek Raida [2], different parameters of ANSA are highlighted. Geometric parameters, optimal surface mesh and Quality criteria of mesh in ANSA for electromagnetic simulation models are determined. M. W. Beall et.al[3], present the different techniques for geometry access for simplification of CAD model for simulations. The techniques are classified in four different approaches as follows a). Translation and healing, b) Discrete Representations, c) Direct Geometry access, and d) Unified topology accessing geometry directly. The paper purposes briefly all broad range of issues face during geometry access. The study done by Geoffrey Butlin and Clive Stops[4] explains dirty geometry problems not suitable for optimal mesh. The study also has detail about repairing and cleaning geometry for analysis purpose. It has highlighted issue related to automatic meshing.

Study done by Andrey A. Mezentsev and Thomas Woehler[5] talk about geometrical and topological errors of CAD model. This study highlights the bad meshing geometry of CAD model. The automated algorithms have applied for automated pre-processing of CAD model by fixing and removing all kind of errors from the model. The study done by S. Dey et al.[6] presents the issues related to automatic identification and elimination of adverse influence of small geometric model features on the quality of automatically generated meshes. M. S. Shephard et al. [7] presents an algorithm to eliminate the adverse effects of small model features at the mesh level. R. Sun et al.[8] purposes a simplification method for boundary representation models (B-rep) using region suppression. The method removes every unwanted region of B-rep model and creates simplified surfaces that cover each supressed region based on boundary loop decomposition of the suppressed region. S. Gao [9] presents feature suppression based CAD mesh model simplification framework. The study has major three steps. First, CAD mesh model is separated by an algorithm called watershed segmentation. Secondly features are extracted by feature recognition method. Extracted features are removed by applying different suitable method as mentioned in paper. G. Foucault et al.[10] purposes Mesh Constraint Topology model with automatic adaptation operators. The approach seeks to transform CAD model into FEM model by decomposing mesh relevant entities (face, vertexes, and edges).

Mesh constraint topology make perfect model for meshing by deletion of edge or vertex, collapsing edge and merging of vertex. A. Thakur et al.[11] have compiled a list of different techniques to simplify the CAD model. The techniques are classified in four categories, 1). Surface entity-based operators, 2). Volume entity-based operators, 3). Explicit feature-based operators, 4). Dimension reduction-based operators. A study done by A. Sheffer[12] suggests the face clustering algorithm to simplify the CAD model for FEM mesh generation application. The technique is based on three steps: Face clustering, finding the collapsible faces and simplification. This technique is semi-automatic; a lot of manual work is done during face clustering. K. Inoue et al.[13] purposes face clustering algorithm for clustering a large number of faces for the purpose of surface mesh generation. They suggest decomposing small faces into large faces by face clustering and generating the mesh on simplified model. At last, all generated sub meshes are merged together to form one mesh. H. Zhu and C. H. Menq [14] specify an approach to remove fillets and rounds from the B-rep models by automatic recognition.

The proposed approach utilizes an incremental knitting process to handle various topological structures of fillets and rounds such as ring type chain and disc type chain to get robust mesh. S. Venkataraman et al.[15] suggests an algorithm for deletion of blends from B-rep model. This paper gives preview complex blend network in detail. The paper shows blend recognition and algorithm to supress the blend from complex structures. The algorithm differs from other blend deletion algorithms due to unique feature. New faces recreate after blend deletion in certain situations by specified algorithm from authors. A.Nogueira et al. [16] have purposed comparison on geometrical simplification with three different models during electromagnetic analysis. The model consisting of very simple wiring harness shows strange behaviour than other two models during electromagnetic analysis. The second and third model shows very much similar results as third model includes car body also. The results are same in last two models, so car body has been neglected during electromagnetic analysis. S.B.Andersen et al. [17] have explained the model simplification of gearless mill derive during FEM magnetic calculations. The investigation is done on simplification's influence on force and torque of derive. S.Savia et al. [18] have developed electromagnetic model of car from CAD data with different simplification stages.

The comparison of simplified models is done after simulations. The more simplified model gives very poor results as compared to another simplified model. S.Feri et al. [19] have purposed overall process to deal with complex model of car during electromagnetic analysis. The pre-processing is done of car body and cable harness to reduce the computational time. J.A.Flint and A.R.Ruddle [20] have presented electromagnetic analysis of car model by applying the different numerical techniques. The simplified CAD model of car has been used. A.R.Ruddle [21] has presented paper about development of vehicle electromagnetics models. It talks about the processing of CAD data, identification of vehicle components that could be neglected from numerical models and computational issues.

The data obtained from the literature provides guidelines for modifying and simulating the CAD models. Therefore, this study will employ the different feedbacks in the literature review in the simulation of the CAD models. This study has presented a hybrid method of simplification of the CAD model which can be proved useful in the present and future as well. The simulation results presented in a treated example highlights the efficiency of the proposed method. The proposed method may serve in future as different advantages. In the simplification process, the input and output files are in a neutral format which is used by the totality of CAD and Analysis tools and systems. It can also ensure the quality of simulation result and makes the process interactive. After treatment, the CAD part is presented by an iso-zone model, so the designer can intervene in the choice of details to be deleted using some criteria. The simplification process is based on a CAD model, the reconstruction process is performed without approximation. A hierarchic link is saved between the initial model and the adapted model, to allow a perfect CAD/Analysis integration. To improve even more the simplification method, it can also consider the orientation of the details compared to the loadings, this criterion will be a subject of future work.

2 Overview of CAE Software

2.1 Process to Build Model for Electromagnetic Simulation

Figure 2.1 shows the cycle for developing a prototype. The process begins with the design of the CAD model followed by the modification of geometries, meshing, electromagnetic compatibility, and the development of the final prototype.

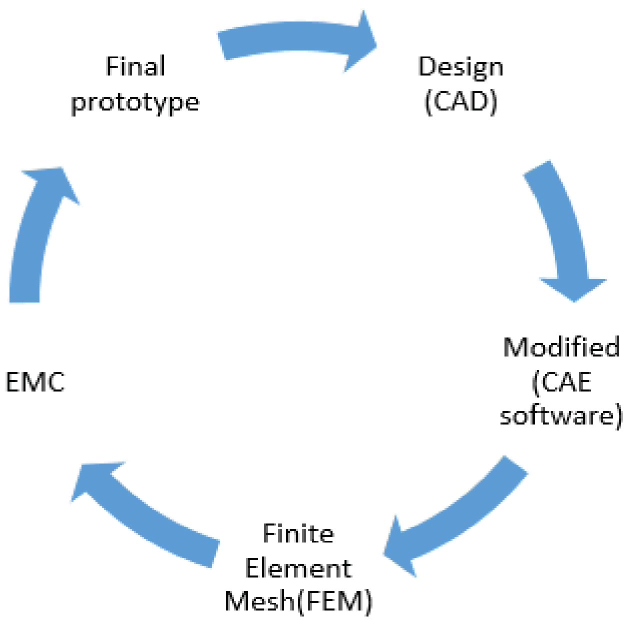

Figure 2-1. Processes for preparing a prototype.

Computer Aided Design (CAD) means to design a model by engineers. Computer Aided Engineering (CAE) uses to analyse the designed model by CAD designers. CAD and CAE are both different terms. CAD model design bases purely on geometrical operations. CAD designer even hide entities which are not necessary during CAD design operation. So, the CAD model has a lot of unwanted and irrelevant details. The analysis cannot be performed directly on CAD model, as it needs modification before applying analysis. Translate CAD model into CAE module and perform simplifications on it. Computational time and quality of mesh depends upon geometric shape of CAD model. As simpler the CAD model geometry is, as less computational time and better quality of mesh in CAE environment. Mostly experienced CAE engineers do not perform initial steps to modify the CAD model for analysis. They consider it less important because it is very time consuming. It takes almost 75 percent to 80 percent time of whole project to rebuild the CAD model and make it suitable for analysis. It is very important to modify the CAD model in CAE environment before analysis because meshing is base of analysis. Meshing highly depends upon how the CAD model is cleaned or modified.

2.1 CAE Software Capability

The CAD model modification is completely depending upon the available software. ANSA [22] plays an important role in this thesis. As the simplification process of CAD model is almost same so we use ANSA mostly to simplify the CAD model. Figure 2.2 explains the various stages for building CAD model using the given software platforms for finite element mesh generation. The whole process interrelates with each other. During working on CAD model, we can jump from first to third stage, while can come back on first or second stage from forth stage. It's totally up to the situation during modification process of CAD model, so we can go back or forward to fix issues.

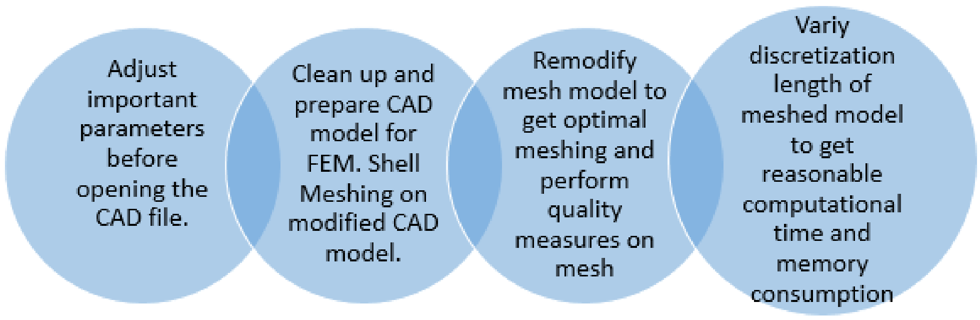

Figure 2-2. Processes for building CAD models using ANSA or HYPERMES platforms [22].

Adjustment of Important Parameters

These following parameters should be adjusted before reading any CAD model.

2.1.1.1 Resolution

The appearance of the visible geometric entities depends upon the resolution values [22]. The user input values apply to all the currently visible entities. The decrease in input value results in higher resolution and vice versa.

2.1.1.2 Tolerances

It is essential for software to cope with changes of its surroundings and remaining functions. In figure 2.3, it is shown that tolerance settings constitute both the Cons and Hot point matching distance. Cons term use in CAE software for boundary or edge which separate two faces from each other. Automatic topology is performed according to tolerances values so there is need to specify appropriate tolerances values before reading the CAD model. The very large or very small tolerance values can cause errors in CAD model as collapsed faces or gaps respectively.

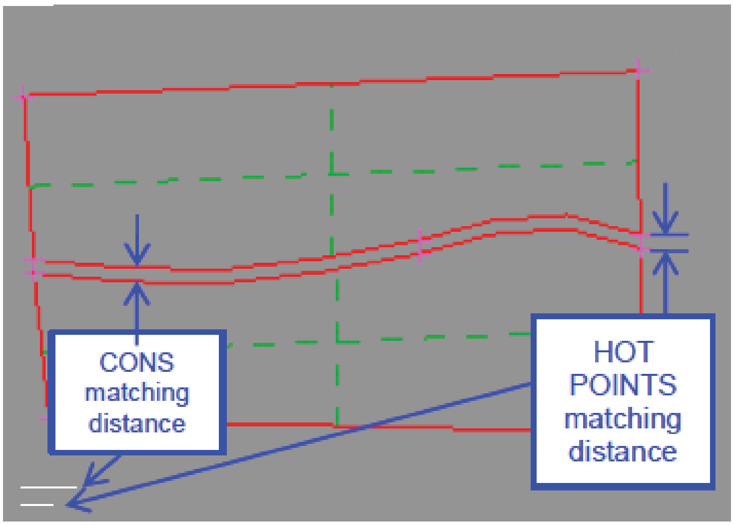

Figure 2-3. Tolerance's settings showing both the CONS and HOT POINTS matching distance. Image taken from [22].

2.2 Repair and Modify CAD Model

2.2.1 Cleaning the CAD Model

The cleaning process is very important to prepare the model for analysis. The software [22] are eligible to locate the topological problems and isolate them automatically. Some errors are not removed automatically; manual repair performs to clean the geometry by user. It takes time to clean the complex CAD model, where manual repair is high. The automatic cleaning can repair overlap faces, collapsed cons, needle faces, Cracks, Small gaps and Unconnected faces. The manual repair needs on triple cons, large gaps, unchecked faces, Irregular face boundaries and untrimmed faces.

2.2.2 Feature Recognition and De-featuring

The features can be recognised, removed or modified base on the requirement of analysis [22]. Holes, fillets, chamfers, flanges and logos are most concerned entities to deal for getting simplified model. These entities can be handled by software automatically. Holes can be removed manually or automatically. Logos isolation can be done to get simplified model by appropriate parameters. Flanges, Fillets and Chamfers can be recognized and modified automatically by giving specified parameters from user to get the desired shape. The geometrical modification is done manually. A geometrical entity modification depends on the analysis requirement.

2.2.3 General Process for Surface Mesh

The robust mesh is very important for an analysis. The accuracy of results depends upon optimal mesh. The mesh consists of TRIA (triangles), QUAD (quadratics) and MIXED (triangles and quadratics). The meshing algorithms depend upon the geometry of model. The more useful algorithms are those which can handle manually [22], because automatic mesh generation cannot generate robust or optimal mesh. The good mesh always requires manual help by user. Batch mesh is most important algorithm available in the software which can generate smooth mesh as compared to other algorithms. Batch mesh can handle difficult geometry while some algorithms are useful only for simple geometry.

2.3 Operators to Improve the Quality of Mesh

2.3.1 Reconstruct

It is applied on already defined surface mesh [22]. It is powerful tool for creation of high-quality surface mesh. It reconstructs the problematic areas and optimizes the overall quality of the mesh according to the mesh parameters. Violating fillets and flanges can improve by this operator.

2.3.2 Reshape

It is applied on meshed macro areas to improve the mesh quality [22]. The advantage of this operator is, it eliminates the need to manually cut, join and align the macro areas of mesh.

2.3.3 Smooth

This operator [22] automatically applies smoothing attributes so as to relax the mesh on already meshed Macro areas.

2.3.4 Fix Quality

This function improves element quality [22] on meshed macros according to all selected quality criteria.

2.4 Mesh Quality Criteria

The following criterion is important for improving the quality of a mesh.

2.4.1 Aspect Ratio

Aspect ratio of two-dimensional elements is calculated by dividing the maximum length side of one element by the minimum length side of the other element. In figure 2.4, the aspect ratio of a triangle and a quadrilateral is demonstrated by dividing the maximum length of the latter with the minimum length of the former. The aspect ratio for the equilateral cell or face (an equilateral triangle or a square) is 1. The value of aspect ratio should be less than 5 but 1 is an ideal value.

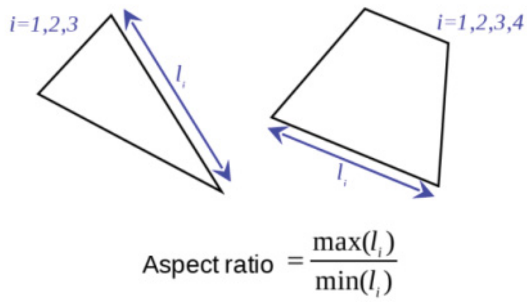

Figure 2-4. Nastran Aspect ratio image taken from [22].

2.4.2 Skewness

Skew in quads is calculated by finding the minimum angle between two lines joining the opposite mid-sides of the element. In figure 2.5, the skewness of a triangles and quadrilaterals is calculated by finding the minimum angle between the vector from each node to the opposing mid-side and the vector between two adjacent mid-sides at each node of the element. The ideal value of Skewness is zero, while acceptable value is less than 45°.

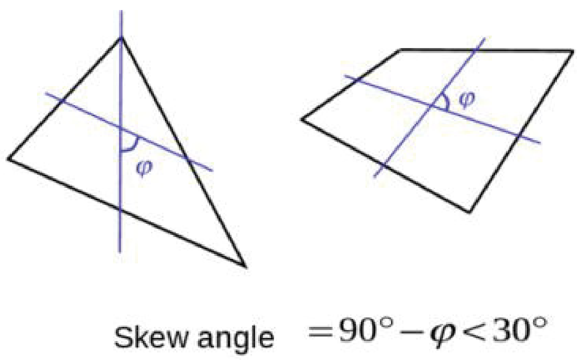

Figure 2-5. PATRAN Skewness image taken from [22].

2.4.3 Minimum and Maximum Element Length

Minimum element length is applied to check the minimum feature length captured and the presence of any zero length elements. If any element length is zero, it means the feature is deteriorating. Maximum length of element, as shown in figure 2.6, coincides with the maximum length of mesh element.

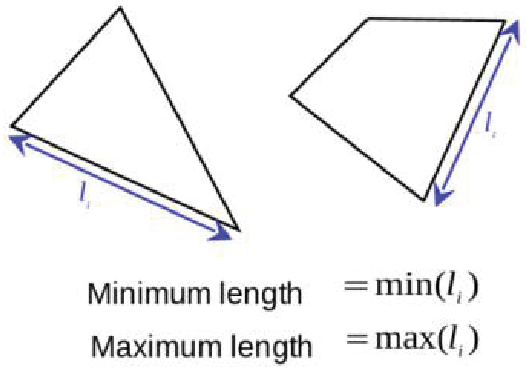

Figure 2-6. Minimum and Maximum Element Length image taken from [22].

2.4.4 Jacobian

Deformation of element from actual shape known as Jacobin [22]. Jacobian gives detail of deviation of element from its ideal shape. Its value ranges from 0 to 1. The value of 1 indicates perfectly shaped elements.

2.4.5 Minimum and Maximum Angle

The angle of quads and triangles are most important in surface mesh quality [22]. For surface mesh, element should be equilateral as much as possible. Equilateral triangle has all three angles equal to 60°. While for equilateral quad all four angles are equal to 90°. So, for triangles ideal value of angle is 60° while for quads the ideal value of angle is 90°. All meshed elements cannot be equilateral. As shown in Figure 2.7, minimum angle of a triangle should not be less 30° while the maximum angle should not be greater than 120°. Similarly, the minimum angle of a quadrilateral should not be less than 45° while the maximum angle should not be greater than 135°.

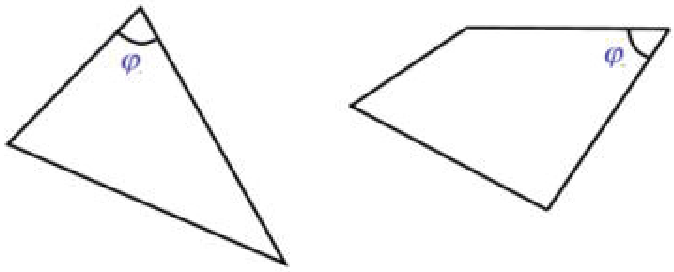

$$\text{Angle} = F_{\min} < \varphi_i < F_{\max}$$

Figure 2-7. I-DEAS Angle image taken from [22].

3 Electromagnetic Theory

Just a single charged particle generates the electric field. Electric field E is electric force per unit area. It is created by differences in voltage. It is directly proportional to voltage. It can be visualize by series of lines called electric field lines. Closer the field lines, means stronger an electric field. Field exists when current is not flowing. When current flows, it creates the magnetic field. The greater the current flow the stronger the magnetic field (B). The direction of magnetic field lines indicates the direction of magnetic field as same case for electric field. The change in magnetic field produces an electric field that itself is changing. This changing in electric field will in turn produce a changing magnetic field. This changing magnetic field will once again produce yet another changing electric field and so on. The net result of changing of both fields $\vec{E}$ and $\vec{B}$ is known as electromagnetic wave. If the voltage source varies sinusoidally than both fields also vary sinusoidally. Both fields are perpendicular one another and perpendicular to the motion of wave. There are different kinds of electromagnetic waves which distinguish in frequency. Electromagnetic wave propagates with speed of light and has same speed in vacuum. As frequency increases, the wavelength of wave decreases. The main purpose of the electromagnetic theory is to provide the study with a platform for analysing the electromagnetic component of the CAD model. The mathematical equation system of the theory will allow the physical phenomenon of the CAD model to be analysed, interpreted, and understood from the perspective and dimension of electromagnetism. The simplification allowed by the electromagnetic simulation enhances the accuracy of the numerical evaluation of the model. The extraction of the results is optimised by reducing work time and prerequisite computational resources. The theory is critical for understanding how radio waves interact with different parts and materials of the CAD models. The main measurement of interest here is the variation of the magnetic flux distribution with frequency in targeted points. This allows the assessment of each part's vulnerability to electromagnetic waves in real life. We are concerned with radio waves in this project which are represented mathematically by equation 3.1.

$$c = f\lambda \tag{3.1}$$

The speed of light is c. Wavelength of wave is λ and it is the distance between two successive crests or troughs of wave. Frequency is f and it is number of oscillations per second.

James Clerk Maxwell purposed set of equations which demonstrate the relationship between electrical and magnetic fields. Maxwell equations play important role for Antenna and electromagnetics. The four Maxwell are equations are following.

3.1 Gauss's Law of Electricity

Electric flux, φ_E, represented by equation 3.2, is the number of electric field lines that pass through the surface. φ_E is zero if all the electric field lines enter the surface from one side and leave from other side. φ_E can only be non-zero if some electric field lines start or end in enclosed region.

$$\varphi_E = \oint \vec{E} \,.\, d\vec{A} \tag{3.2}$$

Gauss's law for electricity says, there will only be flux if the enclosed section includes a net charge. It tells us that electric charge of any shape produces an electric field. In equation 3.3, the closed integral of dot product of electric field $\vec{E}$ and small influential area $d\vec{A}$ is equal to total charge enclosed in chosen surface $Q_{enclosed}$ divided by constant known as permittivity of free spaceϵ_0.

$$\oint \vec{E} \,.\, d\vec{A} = \frac{Q_{enclosed}}{\epsilon_0} \tag{3.3}$$

3.2 Gauss's Law for Magnetism

The numbers of magnetic field lines enter are equal to number of magnetic field lines exit. The net magnetic flux of any closed surface is zero. Equation 3.4, the equation of Maxwell basically tells that magnetic field is different from electric field as it has no beginning and end. We can say, magnetic field lines are continuous. Closed integral of dot product of magnetic field $\vec{B}$ and small influential area $d\vec{A}$ is zero as magnetic flux of chosen surface is zero.

$$\oint \vec{B}\,.\,d\vec{A} = 0 \tag{3.4}$$

3.3 Faraday's Law of Induction

The change in magnetic field will induce an electric field called Faraday's Law of Induction represented by equation 3.5. Close integral of dot product of magnetic field $\vec{B}$ and small influential displacement $d\vec{l}$ is equal to negative of rate of change of magnetic flux.

$$\oint \vec{B}\,.\,d\vec{l} = \frac{-d\phi_B}{dt} \tag{3.5}$$

3.4 Ampere's Law

This law says, as change in electric field can create magnetic field or change in magnetic field can create an electric field. As shown in equation 3.6, the close integral of dot product of magnetic field $\vec{B}$ and small influential displacement $d\vec{l}$ is equal to electric current that is moving some region of space plus change in electric flux with respect to time. This relation is useful for calculation of electric field lines of simple geometries.

$$\oint \vec{B}\,.\,d\vec{l} = \mu_0 I_{enclosed} + \frac{\mu_0 \epsilon_0 d\phi_E}{dt} \tag{3.6}$$

3.5 Relevance of Electromagnetic Theory in Study

The groups Electromagnetic Compatibility (EMC), Antennas and Tuners within Research and Development perform both physical testing (measurement) and virtual testing (simulations). Virtual testing starts at early stages in design process of new CAD models. Basically, virtual testing addresses problems included electromagnetic emissions, electromagnetic immunity (to external fields), and undesired crosstalk between cables, components, and/or antennas, and optimal antenna placement on cars. The problems range over both high and low frequency domains. Therefore, electromagnetic waves with low frequency domains are applied on CAD geometries in this thesis for analysis purposes. The behaviour of original and modified CAD geometries has been notified by performing Electromagnetic analysis.

The problem of Electromagnetic analysis on a macroscopic level is the problem of solving Maxwell's equations to certain boundary conditions. Maxwell's equations are a set of equations, written in differential or integral form, stating the relationships between fundamental electromagnetic quantities. One of these electromagnetic quantities is magnetic flux density B. The behaviour of magnetic flux density B is observed across whole CAD geometry.

The Maxwell equations are in differential form in RF module of COMSOL Multiphysics. This is because it leads to differential equations that the Finite Element Method (FEM) can handle.

3.6 Electromagnetism and its interpretation in the Present world

The rapid development of computer hardware in recent years provides vast resources for the design of electromagnetic devices. Comparable progress in CAD software has to follow to exploit these possibilities. The advent of CAD methods revolutionizes the design procedure by bringing the analysis of the electromagnetic field in the devices to the foreground. Which provides an insight into their operation far superior to that obtainable by traditional network considerations. The field analysis methods of two-dimensional models can be regarded as established; successful CAD software packages are commercially available. The situation, however, is different with three-dimensional models: their use is by far less widespread. The reason is no longer the considerably higher memory and CPU-time requirement since this is not essential in an age of cheap memory and fast computers. The main problem is the scarcity of robust and reliable numerical field analysis methods. The present work attempts to make up for this shortage.

Today, numerical techniques are a normal tool for professional engineers. The finite element method, together with the finite difference and boundary integral method, are well known. The finite element technique is the most popular for calculating electric and magnetic fields. Originally, it has been developed for analysing mechanical stresses in structures. Its use has been limited due to the lack of computer capabilities. Only by the introduction of powerful workstations, it became possible to practically apply this technique. The theoretical background of the finite element method is found in many papers and textbooks. The user should only be aware of the fact that the system to be analysed is subdivided into a large number of small finite elements. In a two-dimensional analysis, mostly triangles are used. In a three-dimensional analysis, a large variety of elements is found: prisms, tetrahedrons and even more difficult substructures. Instead of using difficult trial functions for the solution of the field in the overall structure, simple formulae are used in a very small portion. Therefore, the mathematics involved become very simple: a set of simple equations with a large number of variables. This is a task a digital computer is very well suited for: handling a large number of simple problems. In the simple approach, the so-called first-order elements are used, in which in individual elements the function is approached by a straight line. In more elaborate systems, second, third, fourth or higher-order polynomials are introduced. The calculated values match the real solution better when more elements are used. High order elements also allow increasing the accuracy, without using a finer division of the geometrical structure. The required calculation time in two-dimensional problems is approximately proportional to the square of the number of elements used. Second-order elements require the same computing effort as four first-order elements, third-order elements can be compared with eight first-order elements. The detailed procedure for solving the equations is of no interest to the user. Internally a set of linear equations is generated, that is solved iteratively. If non-linearities are present, a Newton-Raphson iteration is built around the solution. The required calculation time is relatively limited: a fully equipped personal computer is generally sufficient for solving a full-sized two-dimensional problem in minutes. General considerations in CAD in magnetism Although the mathematical background of the finite element method has been established some seven decades ago, and it has been possible to implement the technique on the computers available in the sixties and seventies, it has been only recently that the finite element method has found its way to the everyday engineering practice. This is due to the time involved in introducing a large amount of data. The batch-oriented mainframe computers of the sixties and seventies were not well suited for engineering work. The introduction of engineering workstations in the eighties gave professional engineering a useful platform. Instead of defining the geometry in an alpha-numerical way, he can draw his geometry as he is used to. After defining the geometry, a semi-automatic or fully automatic mesh generation system is started. After calculating the field distribution, graphical routines are used to interpret the results. A CAD system for calculating electrical and magnetic fields generally comprises three steps which involve problem definition; - solving the problem; - interpretation of the results. This division into three steps is not typical for electric and magnetic field calculations but is also found in other calculations using the finite element method in particular, or more general, using numerical solution techniques (thermal, mechanical, flow problems). The problem definition starts from the geometry of the system. The geometry maybe two or three dimensional, depending on whether a two- or three-dimensional analysis is carried out. Then the structure is subdivided into finite elements. This may be done in an automatic or semi-automatic way. Generally, it is also possible for the user to adapt the automatically produced mesh by the band. After defining the mesh, the materials are linked with the various substructures. Material characteristics are stored in a material library. Non-linearities are no problem. Anisotropy may be taken care of. Apart from the geometry and the materials, the sources have to be defined: - currents and/or voltages in magnetic problems; - charges and/or voltages in electrostatic problems; - currents and/or voltages in steady-state current flow problems.

4 Modification of CAD Models

4.1 Process to Build Model in ANSA

The modification of the CAD models is essential for enhancing their quantification and visual aspects. Generally, shape modification scenarios of object models require precise location and elaboration of errors to facilitate their consistent and coherent correction. The ANSA and HYPERMESH software provide dynamic environments for manipulating geometries and topologies with wide range of property definitions. Their environments are user friendly with high productivity and performance quotient. The key features that make ANSA and HYPERMESH tools of choice for most users include integrated search engine, customizable GUI, rapid function access, dynamic modification and filtering capabilities, and lists handling. The platforms support scalable, centralized, hierarchical, and structured data management which increases the efficiency and effectiveness of data handling. The performance of the two platforms is accentuated by versatile integrated tools that support process automation, identification of geometrical differences in multiple models, and controlled volume and shell meshing. The modification of CAD model in both ANSA and HYPERMESH software follow a similar hierarchical order shown in figure 4.1. The modification of the model can begin with either the elimination of the topological errors or geometrical errors

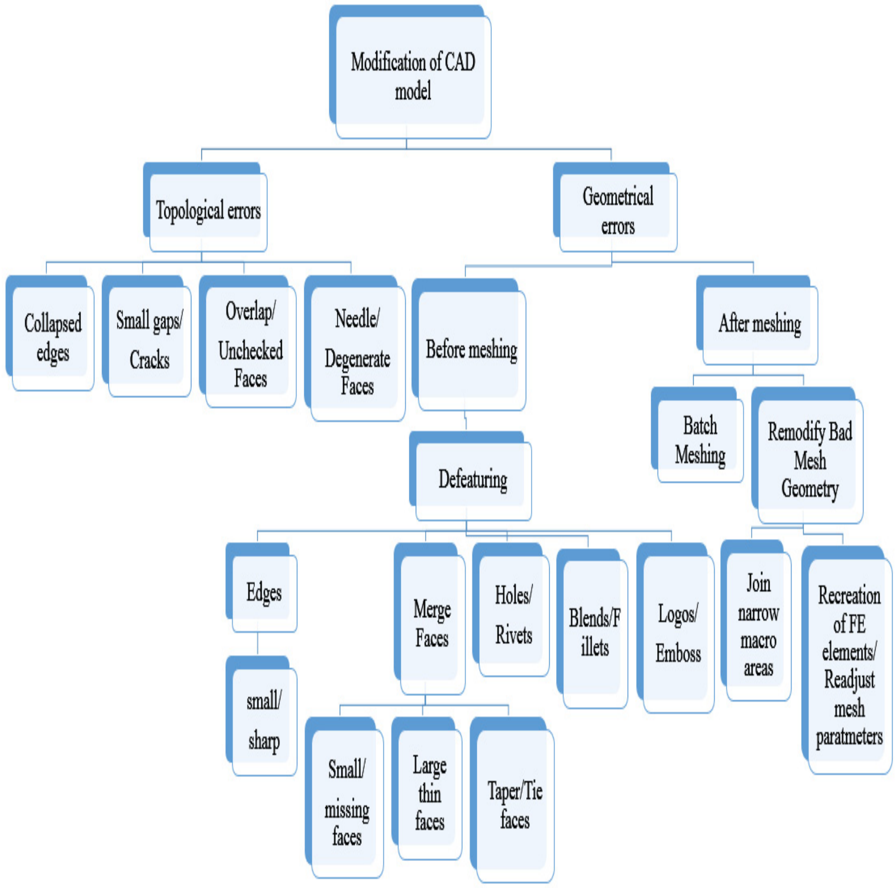

Figure 4-1. Defeaturing CAD model in ANSA.

4.1.1 Topological Errors

All the topological problems cause increase in computational time and decrease in accuracy. These errors generate poorly shaped and over densified elements. It is very necessary to remove these problems to make model clean. For topological errors, first set the resolution and tolerances according to CAD geometry. Then import the CAD file in ANSA and perform geometry clean-up. It can fix topological errors automatically but manual support is required to remove all the topological errors. There are three kinds of edges known as cons in the ANSA. Free boundary of face is known as red cons or single cons, while the common boundary of two faces is known as yellow cons or double cons. Common boundary of three or more than three faces is called cyan cons or triple cons.

4.1.2 Automatic Fixing of Topological Errors

The automatic function of ANSA is Clean G. it works on current given tolerances values. It removes topological errors in huge number including cracks, gaps, needle faces and other topological problems. Topological problems which do not fix by this function are solved by manual process, as some are given below.

4.1.3 Remove Unwanted Free (red) Edges

Make sure single cons are only at free edges of the part or at inner perimeters. If on any other location of part are single cons, they should be removed. We use paste cons function from TOPO menu to remove single cons manually. Faces>Topo function from same menu is automatic process. If cons lie in a distance that satisfy the tolerance values, Faces>Topo will perform all necessary topological actions to the related cons. This function is very fast than manual process. After that we make sure by deactivating double cons, if there remain any single cons.

4.1.4 Collapsed Cons

These are white dots on model. White dots mean cons whose ends are coincident. This problem we face after opening the CAD model. It can occur during repairing the geometrical errors. All cases of collapsed cons are treated one by one. It is very time-consuming process. We use cons>release function to free the double cons. After this function, double cons are converted into single cons. Now delete extra Hot points from single cons by Hot points>delete function. If the gap is more than tolerances specified values, then manually all cons are pasted together one by one. Two horizontal cons near to each other can be pasted together into double cons by Cons>paste function. If cons distance is just under tolerances specified values than only Face>Topo function applies and fix the issue. After fixing the issue only double cons should be visible without white dot.

4.1.5 Triple Cons

The existence of degenerate faces causes the triple cons in model. We delete the degenerate faces, triple cons problem also vanished.

4.1.6 Collapsed Faces

The face whose width remains smaller than tolerances values known as collapsed face. Delete this face and merge this face with connected face by creating new face. After that check topology to make sure problem is solved.

4.1.7 Geometrical Errors

The geometrical errors are removed in two ways. One before doing mesh and the second is after the meshing. The small features and irrelevant features are removed before meshing. While after meshing, the areas which show distortion are removed. At the end goal is to get smooth and optimal mesh.

4.1.8 Before Meshing

The CAD model simplification depends upon the smooth mesh. We remove all the features that are unnecessary for electromagnetic simulations and simplify the complex faces by merging them to get suitable faces for mesh generations. All the feature simplification determined below are performed manually. Manual feature simplification takes time to get ideal model.

De-featuring

The small features which are not necessary for analysis are removed from CAD model. The purpose is to get the smooth geometry to generate the robust mesh on model. There are different entities which we want to remove from model and how to remove them is given below.

Holes and Rivets

Holes are selected manually or automatically. The user specify diameter. All the holes or any circular opening under specified diameter got selected automatically. Then just close these openings. The diameter can be increased to approach the large holes or gaps and fill them. The smooth face obtains after removing any kind of openings. The hole can be selected manually and filled. It takes too much time, if there are large numbers of openings.

Logos

We get idea of the size and height of logos by measuring tool. ANSA removes Logos by giving maximum height and maximum size. The logos come under given range of height and sizes are isolated automatically. The height and size values can increase or decrease to get rid from the logos.

Fillets

Small fillets create very dense mesh, that the reason they should be removed. The small fillets are removed by giving radius. The maximum radius is specified by user and ANSA detects all the fillets under that given radius. The unwanted or unconnected fillets are deleted.

Merge Faces

The faces are merged together to get simple and smooth faces. There is different type of faces, which after meshing cause distortion and small elements. Faces group in TOPO module of ANSA helps to readjust the geometry by modifying the taper, thin, small and missing faces. The unwanted faces are deleted. The new faces are created based on the function Faces > new. The more suitable surfaces are created by this function. Once the surfaces are created, faces are automatically created.

4.1.9 After Meshing

The problems can occur after mesh. The messages show the types of problem that have occurred. Bad face in macros is problematic message appear after meshing. Which means cleaning is not done completely, so go back and do the cleaning process again and re-mesh. X-macros remain unmeshed is another problematic message appear. The solution of this problem is to change the discretization length or change the meshing algorithm. The macro areas can be cut into small, less complicated macro areas to ensure meshing. Narrow macro areas lead to generate elements with high aspect ratio. Macro areas with sharp angle lead to create highly skewed elements. Improve macro areas by joining together to make wider macro area. Then re-mesh it. The macro area can be split into two by cutting it. The finite element violates the desired criteria, can be recreate or split etc. Element penetration can be checked. The quality criterion is very effective in ANSA. There are different ways to check quality measures and take steps accordingly to remove violations. The mesh discontinuities can be monitor if present in model and remove them.

Batch Mesh

The batch mesh is very useful in fixing erroneous elements. It is automatic process. It takes very less time. The manual work reduces by applying this algorithm. We set the desired criteria and run the batch mesh. The two important features are influenced by batch mesh are mesh parameters and quality criteria. Mesh parameters tab fixes violating shell elements automatically. It handles de-featuring which joins parameters automatically come under$\frac{2}{3}\boldsymbol{L_{min}}$. $\boldsymbol{L_{min}}$ is minimum element length to mesh. It handles nodal movement of meshing. It allows the maximum nodal movement from surface during mesh fixing has relation$\boldsymbol{0.05L}$, where $\boldsymbol{L}$ is target length of element for mesh generation. Maximum allowable nodal movement form perimeter has relation $\boldsymbol{2L_{min} - \frac{3}{4}L_{min}}$. The fillet treatment can be done by measuring the radius and width. This is upon the measurement value how to behave with fillets. They can be sharpened, split or how many rows of elements will be created. In the case of flanges set the width range. The number of rows of elements is created according to the width. For the small width, a smaller number of rows of elements, while for higher width, a greater number of rows of elements. Chamfers are given values of angle and width. The treatment is sharpened or split of chamfers.

4.2 The most useful tool used in present times

Today, simulation engineers like Petr Nekolny at Valeo Autoklimatizace K.S. have found a way past the bottleneck of geometry preparation, allowing them to leverage simulation in the product design process: Simcenter STAR-CCM+ again brings us the potential to shorten development time and costs without the need for additional designer effort to prepare specific geometry for simulation.

Thanks to game-changing geometry preparation tools such as 3D-CAD, surface wrapping, and automated meshing, the route from CAD to flow simulation with Simcenter STAR-CCM+ has never been simpler, with manual repair tasks eliminated from the process.

Importing a CAD model and understanding the assembly and design can feel like being dropped into the middle of a corn maze, without any resources to navigate the trails. Luckily, 3D-CAD offers a complete set of tools in the visibility toolbar to quickly understand and organize the geometry.

Let's start by importing the entire business jet model, which is 16455 bodies, into 3D-CAD. The "section view" and "exploded view" can help you understand, visualize and select the enclosed and challenging parts to view. You can "tag" all fuel system bodies and then use filters to hide them and delete the rest of the model. While importing a native or neutral CAD file from another tool, you may well uncover errors in the geometry, and it can be challenging to identify most of them. This is around the time you may begin wishing for a magic wand to find and fix the issues. Even better than a magic wand is the 3D-CAD search tool**,** which allows you to identify the model's invalid bodies or faces.

Out of 222 bodies in the fuel tank model, the search tool can automatically identify 28 invalid bodies. The best practice is to fix these invalid bodies with automatic CAD repair operations like "Repair Body" or "Repair Face", trying to fix and heal the geometry automatically. If an automatic heal fails, you can use CAD repair tools to fix the invalidities. Production-ready geometry typically contains gaps, interferences, fasteners, and tiny features. These features are often necessary for manufacturing but add unnecessary complexity for simulation.

3D-CAD can help here too! The search tool allows you to prepare the geometry by finding similar bodies or topologies like fasteners or unwanted pockets for easy removal, as well as detecting and visualizing clashes or gaps – easily fixed using the extended solid operation. The advanced defeature options allow removing unwanted components with just a few clicks. For flow simulation, the 'wetted surface' needed is usually either the external volume surrounding the geometry or an internal fluid volume. In the case of the fuel tank model, unite all the internal bodies and subtract them from the tank volume. Once the flow domain is created, the (historically) hard part is done. All that remains is to add a single automated mesh operation in the mesh pipeline to generate the surface and volume mesh. the whole process, from geometry import to fluid volume extraction, was done in the 3D-CAD modeller, the sequence of operations was stored and is easily re-executed on the new CAD files in just a few clicks. With the 3D-CAD modeller, the entire geometry preparation and parameterization process is captured as an operation pipeline. Any update or design change can be accommodated with minimum manual effort. Users can quickly set up and evaluate many operating conditions and designs with just a few clicks using a built-in design exploration feature called Design Manager. To design better-performing products and beat your competitors to market at the same, you need to be able to move from running one to hundreds of simulations at a time.

In the case of a better design of the pump, the biggest challenge is to get a realistic, yet robust, parametric definition of the impeller blades. Again 3D-CAD features like 3D-Sketch, loft, and extend solid allow to create of the parameterized blade. Adding Design Manager allows running multi-objective optimization with a parametric impeller for better performance gains. The design Manager was able to find several designs that performed better than the original design in one or both of the output objectives of Head and Efficiency. It turns out that this is about much more than overcoming a bottleneck in the simulation process. It is about unlocking the power of simulation. Using a fast, robust, and repeatable geometry preparation process in 3D-CAD, you can now spend more of that valuable engineering time on just that – finding better designs and delivering value for your business.

4.3 Process for Modifying CAD Geometry

First of all, CAD geometries are short listed to modify for analysis purpose. At start of thesis, complex and large size CAD geometries were prepared for analysis purpose. The selection of CAD geometries was done depending upon the computing system capacity. Total four CAD geometries are analysed for electromagnetic simulation in this report. CAD geometry with flanges is only large size geometry which is included in this thesis for analysis purposes. While other three CAD geometries are with fillets, with hole of 20mm diameter and with holes of different diameters up to 12mm. The small size geometries are used with mutual concern of supervisor and decision is purely based on available computing resources in given time.

The major portion of simulations is done on 64-bit operating system computer, with RAM of 8 GB and Processor of 2.90 GHz. RF module in COMSOL Multiphysics is used to perform simulations in this computing system.

The CAD geometries have been mentioned with two terms in this thesis original and modified. Original CAD geometry has been meshed in ANSA without any change of original shape, while modified CAD geometry is smooth CAD geometry without particular CAD entities like Flanges, Fillets and Holes. After removal of entities, mesh is generated in ANSA on modified geometry.

After meshing in ANSA, both original and modified geometries are transferred on Nastran format. These Nastran files are exported from ANSA. The Nastran files of both orginal and modified CAD geometries are solved in COMSOL. The interfaces in RF module of COMSOL form a complete set of simulation tools for electromagnetic simulations. The frequency domain interface with electromagentic waves in RF module is used in this thesis. The geometry consists of a steel sheet part surrounded by a spherical region of air. The source is a point magnetic dipole placed close to the sheet. Thickness of sheet is constant for each geometry. Simulations are done for a number of different frequencies. Magnetic flux density (B field) is evaluated on different points close to the sheet. One CAD geometry with flanges is simulated in CST, while other all geometries are simulated in COMSOL with RF modules.

5 Results

The following section presents results of different CAD models. Electromagnetic simulations have been performed for a simpler modified geometry and an unmodified geometry. Results are compared for the unmodified and modified geometry with regard to

a. Number of elements.

b. RAM used for solving.

c. Simulation time.

d. B field in 3 points.

5.1 Reference CAD Geometry with Flanges

Original CAD Geometry with Flanges

Figure 5.1 shows the original/ reference CAD geometry with flanges. There are small details including flanges in original geometry.

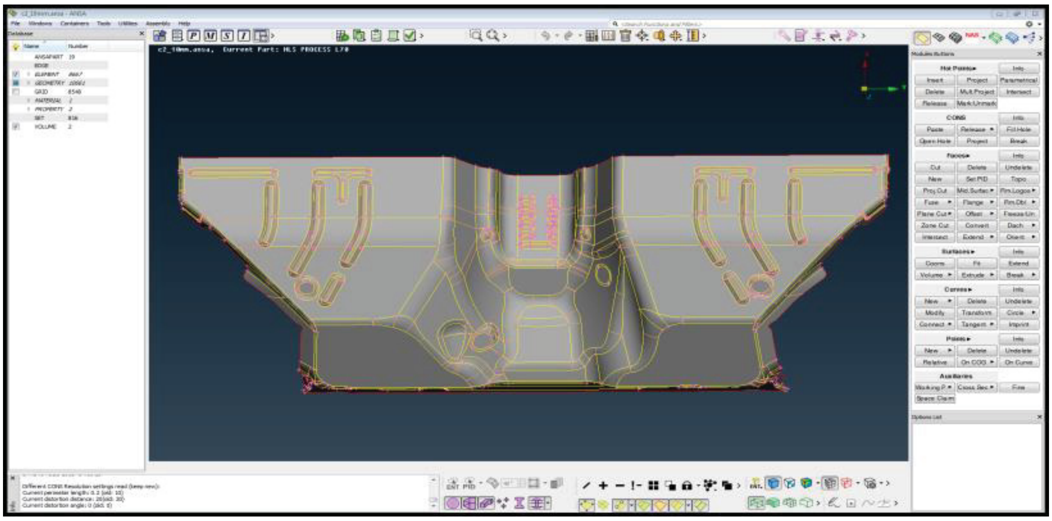

Figure 5. 1. Original CAD model in ANSA with Flanges

Original CAD Geometry after Meshing

Figure 5.2 shows the original CAD geometry after meshing.

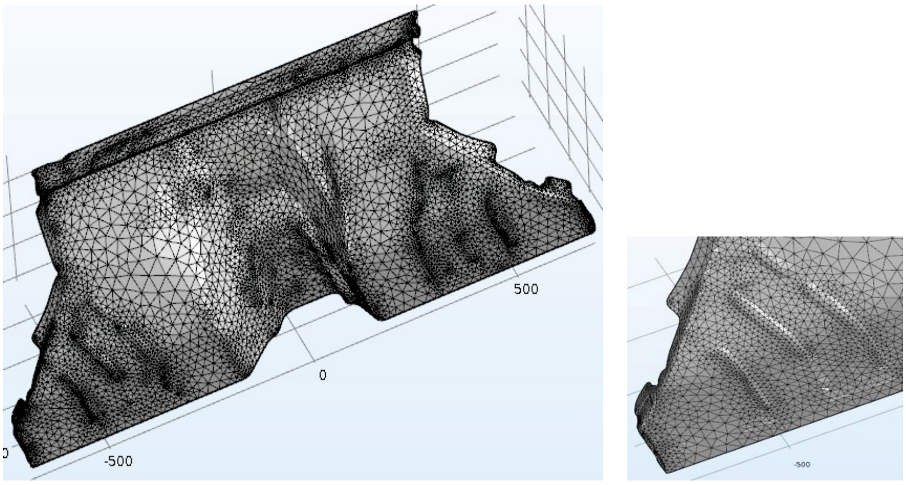

Figure 5. 2. Original CAD model with Flanges after meshing.

Modified CAD without Flanges

Figure 5.3 shows the modified CAD geometry without flanges. Flanges and other small details are removed form Modified CAD geometry as showed below.

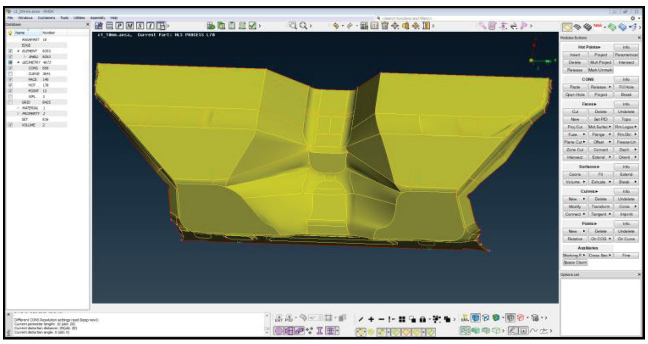

Figure 5. 3. Modified CAD model in ANSA without Flanges.

Modified CAD Model after Meshing

Modified CAD geometry is meshed as shown in Figure 5.4. Geometry is cleaned up, no wanted edges inside. Therefore, mesh looks rather smooth and regular because the analysis is based on mesh and mesh quality.

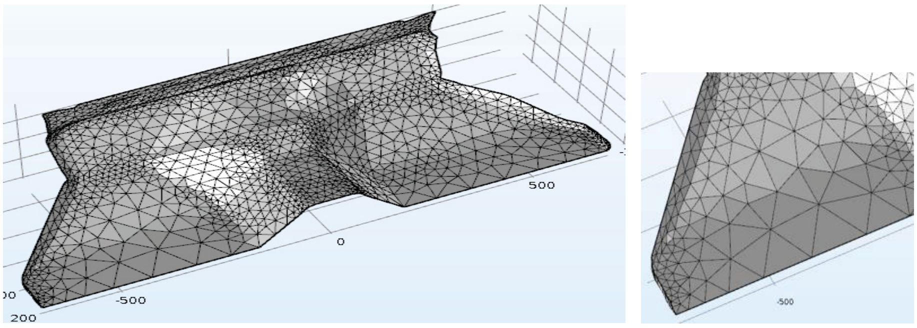

Figure 5. 4. Modified CAD model without Flanges after meshing.

Point Magnetic Dipole

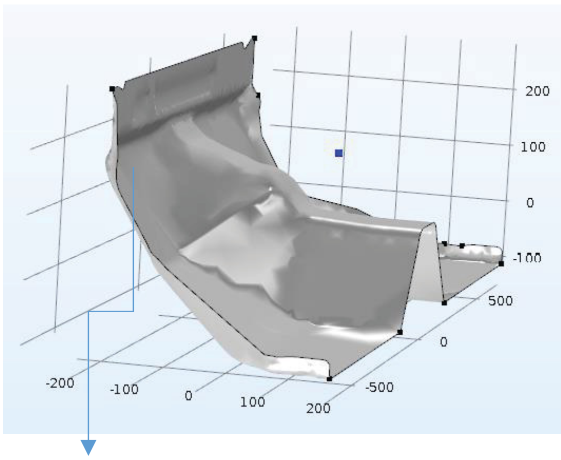

Figure 5. 5. Point magnetic dipole used as source, 1 Am2 in vertical direction.

Point magnetic dipole shown in figure 5.5 is used as a source in vertical direction. Magnetic field is registered at three different points as showed in Figure 5.6. Magnetic flux density has been presented for three points in Table 5.2. Nine Frequencies applied with varying ranges from low to high sequence, also mentioned in Table 5.2. Now values of both geometries are compared to find accuracy. Accuracy can be compromised up to 5% to get desired results.

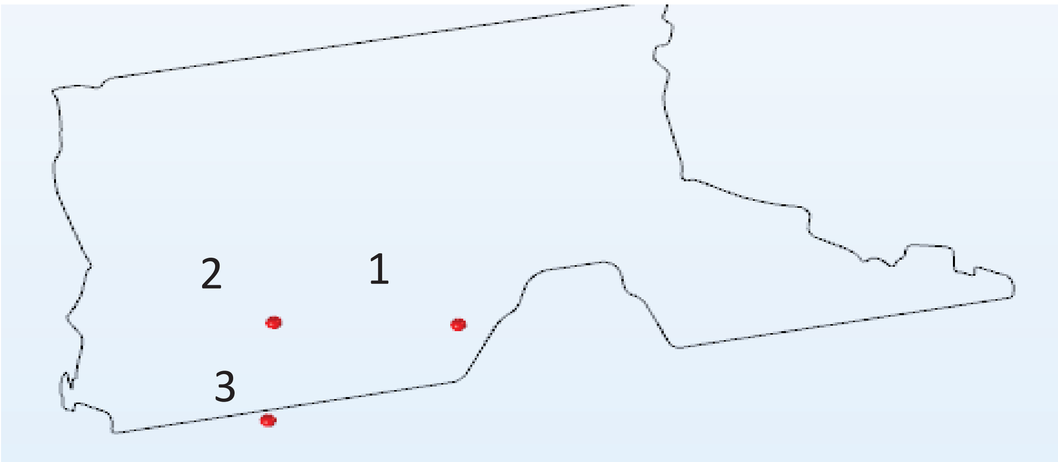

Figure 5. 6. Locations where the B field is registered.

Axis used for three points mentioned in Figure 5.6 are (0, 0,-100), (140, -400, 0) and (140, -400, -150) respectively.

Three variables, Simulation time, Memory Consumption and number of elements are presented in Table 5.1.

Table 5.1: Solution details of original and modified CAD geometries.

Original CAD Geometry	**Modified CAD Geometry**
Tetrahedral elements: 218788	Tetrahedral elements: 59787
Triangular elements: 15178	Triangular elements: 4659
No. of DOF solved for: 1455900	No. of DOF solved for: 395798
Solution time: 3197 s	Solution time: 879 s
Physical memory: 7.98 GB	Physical memory: 4.98 GB

Table 5.2 presents a dataset for electromagnetic bi-polar field variations for three points on reference and modified CAD models for radio frequency band between 100Hz to 1MHz. The data demonstrates that electromagnetic exposure for each part of the model changes with variation in the frequency of the radio waves. Radio waves with low frequencies have higher B-field values than those with high frequencies. The six points were selected because they hand the highest magnetic flux density on their respective CAD models.

Table 5.2: B-field [µT] vs frequency [Hz] in three locations for Original and modified geometry.

	Unmodified			Modified		
Frequency	Point 1	Point 2	Point 3	Point 1	Point 2	Point 3
100	5.7043	1.7064	1.1099	5.7182	1.7269	1.1242
1000	1.3014	2.0312	0.8444	1.2923	2.0527	0.8629
10000	1.2590	2.0611	0.7018	1.2426	2.0825	0.7092
100000	1.0770	2.0719	0.6253	1.0613	2.0989	0.6218
300000	0.9477	2.0822	0.5648	0.9310	2.1109	0.5566
1000000	0.6523	2.0750	0.4557	0.6355	2.1040	0.4437

3000000	0.3685	1.8722	0.3361	0.3535	1.9022	0.3226
10000000	0.1290	1.2226	0.1411	0.1211	1.2446	0.1316

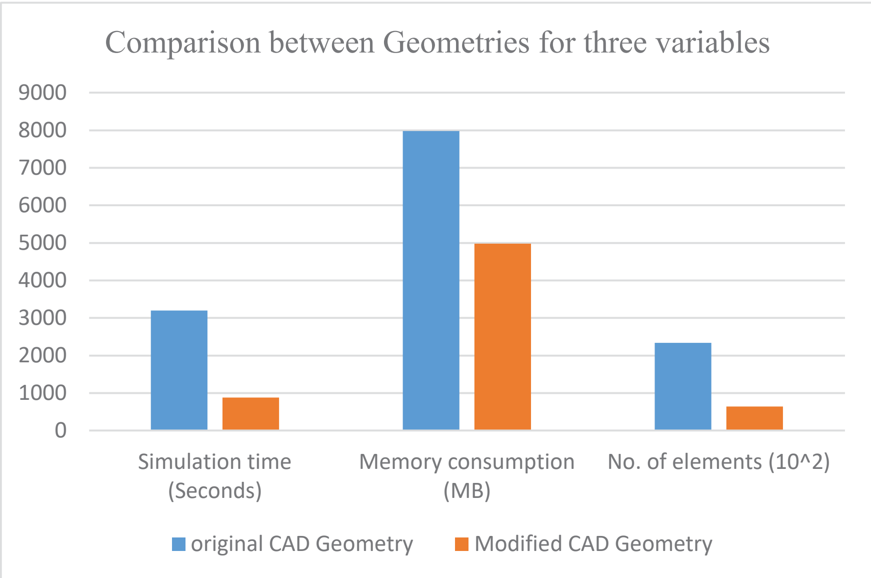

Figure 5. 7. Differences between the original and modified geometries for Flanges.

Original CAD geometry has high bars in all three variables as compared to Modified CAD geometry, shows in Figure 5.7. The number of elements after meshing is 72.45% less in Modified geometry as compared to the original geometry while 37.59% less memory is consumed in updated geometry. Simulation time in original geometry is 72.5% more than other modified geometry. Magnetic flux density flow chart is presented in Figure 5.8. In Figure 5.9, it is shown that there is limited difference in magnetic flux density flow in both geometries. Overlapping shows accuracy is compromised only less than 2%. Analysis for geometry removing flanges showed good results in terms of saving computing time and memory consumption. Flanges can be removed to get fast computing results. Accuracy is compromised very less. That means CAE engineer can save a lot time during simulation. Frustration of system crash during computation can be avoided by removing flanges from complex CAD geometries like passenger car CAD models. This can help to perform the EMC analysis successfully for very complex geometries of passenger cars.

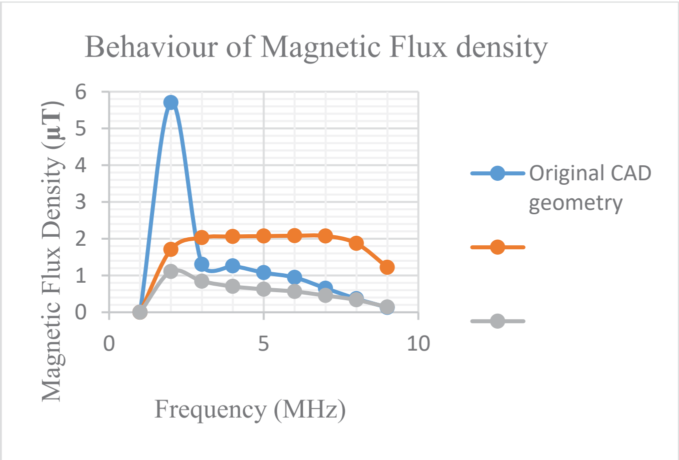

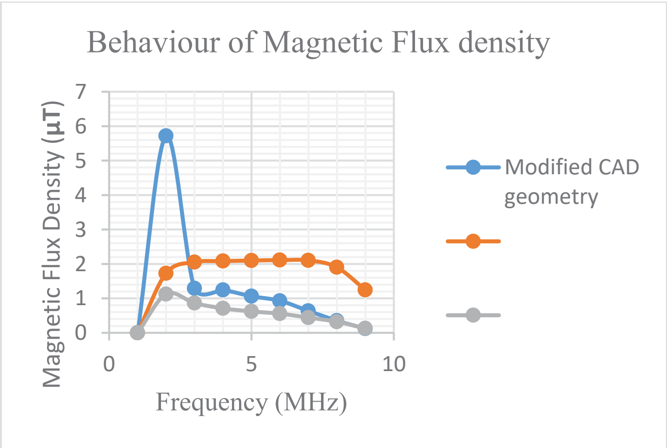

Figure 5. 8. Frequency vs Magnetic Flux density for Original and Modified CAD geometry for Flanges.

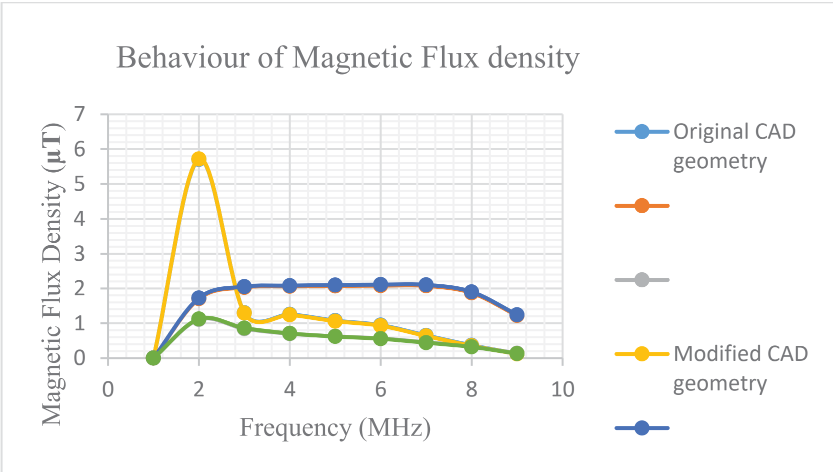

Figure 5. 9. Overlapping of solution of both Original and Modified CAD geometry for Flanges

5.2 CAD Geometry with Fillets

The CAD geometries shown in Figure 5.10 have fillets and smooth surface respectively in ANSA. Original CAD model had 13 fillets of different diameter and width which were removed to get smooth surface for analysis purpose in modified geometry.

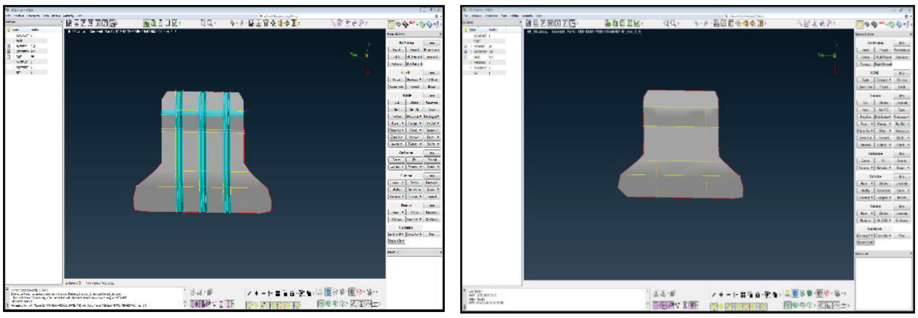

Figure 5. 10. CAD model with and without Fillets in ANSA.

The finite element mesh is generated on the both models with different discretization lengths. The Target length of mesh varies from 15mm, 6mm and 3mm. The main purpose is to find computing time and memory consumption with suitable mesh by compromising accuracy less than 5%. An error margin of 5% is an acceptable number because it allows designers to have greater control over product designs without interfering with product dimensions and development process. The reason to use different target lengths is to get desired results by generating reasonable mesh. Therefore, it has started with a coarse mesh to dense mesh and understands the modelling results. Then use a finer mesh if needed.

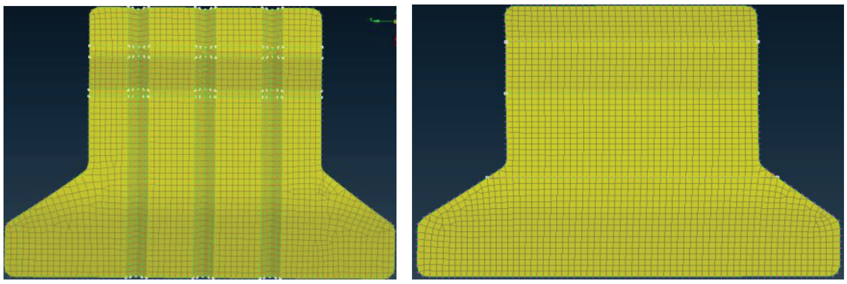

Figure 5. 11. Meshing in ANSA with and without Fillets.

The CAD geometries shown in Figure 5.11 are exported as Nastran from ANSA. Nastran files are converted into STL files. STL files are opened in COMSOL. RF module with electromagnetic waves is applied in COMSOL.

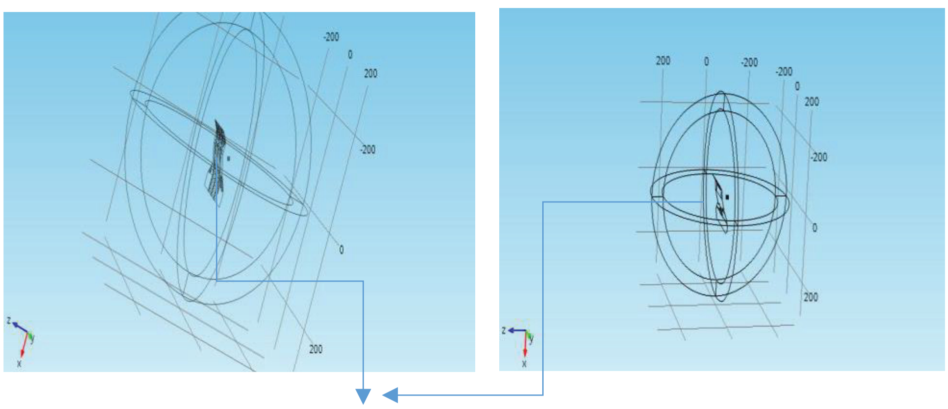

Figure 5. 12. Magnetic point dipole on geometries with fillets and without fillets in COMSOL respectively.

The magnetic point dipole is fixed on both geometries as shown in Figure 5.12 at different positions call Cut point 3D. The analysis is performed in COMSOL for both geometries with and without fillets on different locations by adding cut point 3D. The magnetic point dipole is fixed on both geometries as shown in Figure 5.12 at different positions call Cut point 3D. The cut points 3D are set at 20mm, 30mm, and 80mm for the x, y, z coordinates respectively. The analysis is performed in COMSOL for both geometries with and without fillets on different locations by adding cut point 3D. Magnetic flux density distribution on each cut point 3D is analysed. Each geometry has been analysed from coarse to dense mesh with target lengths of 15mm, 6mm and 3mm respectively. The solution is presented in Table 5.3 and Figure 5.14. Frequency domain remains constant for each analysis. A total twelve Frequencies are used for solution presented in.

Table 5.3: Meshing and Simulation results for geometries with fillet and without fillets.

Geometry	Number of Faces in geometry	Finite Element Mesh Generation in ANSA		Simulation in COMSOL		
		Target Length (mm)	No of elements	Simulation Time (Seconds)	Memory Consumption (Mb)	No. of DOF
Without Fillet	112	15	96	1212	1775	95876
		6	596	1422	1927	111546
		3	2298	2037	2571	131790
With Fillet	15	15	98	1387	1890	106986
		6	635	2215	2580	135410
		3	2362	3188	4500	263144

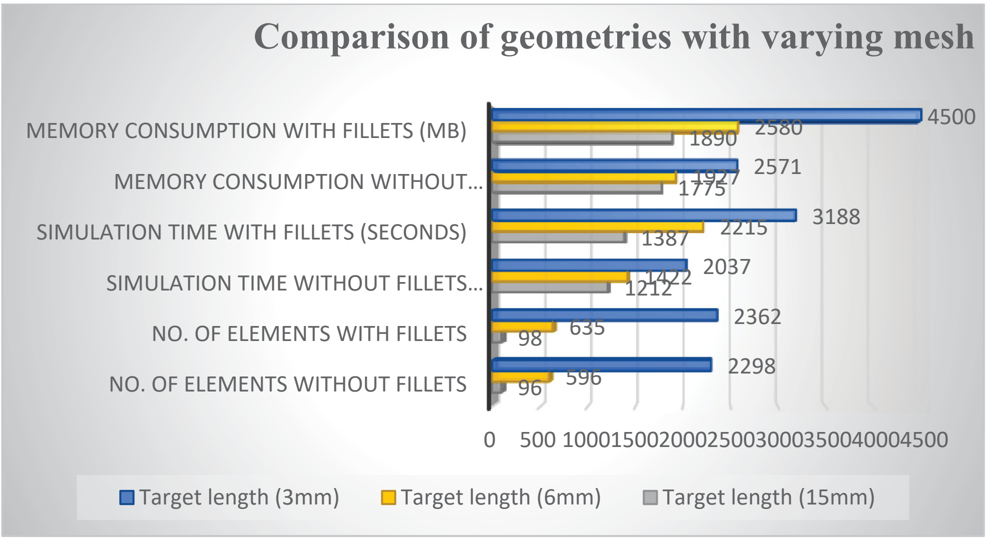

Figure 5. 13. Fillets and without fillets geometries solution comparisons with different target lengths.

The number of elements is higher after meshing in original CAD geometry as compared to modified one, as shown in Figure 5.13. The greater number of degrees of freedom need to be solved for geometry with fillets. Therefore, simulation time and memory consumption are higher in geometry with fillets.

Table 5.4: *Frequencies range used during EMC analysis in COMSOL.*

Frequency (Hz)
3e5
2.8e6
5.3e6
7.8e6

Frequency (Hz)
1.03e7
1.28e7
1.53e7
1.78e7
2.03e7
2.28e7
2.53e7
2.78e7

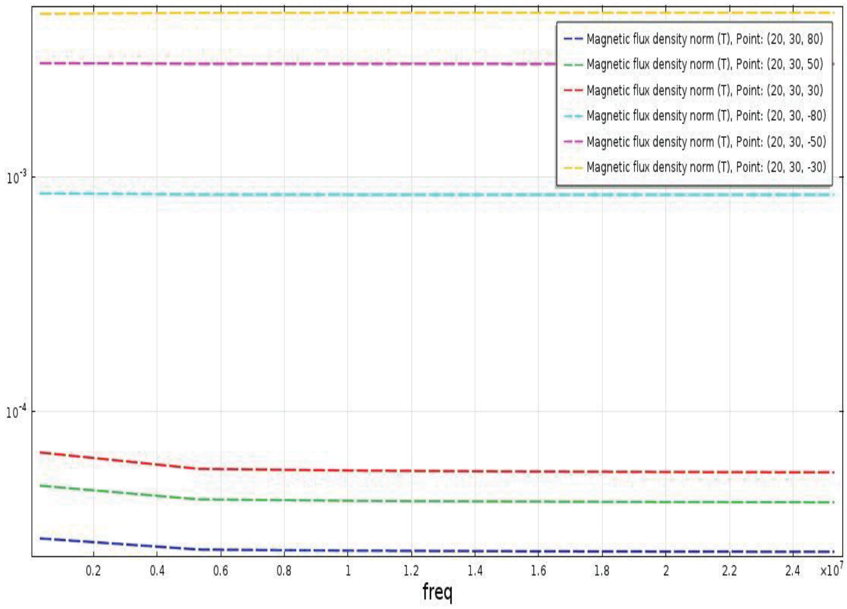

Figure 5. 14. Frequency (Hz) vs Magnetic Flux density for geometry with fillets.

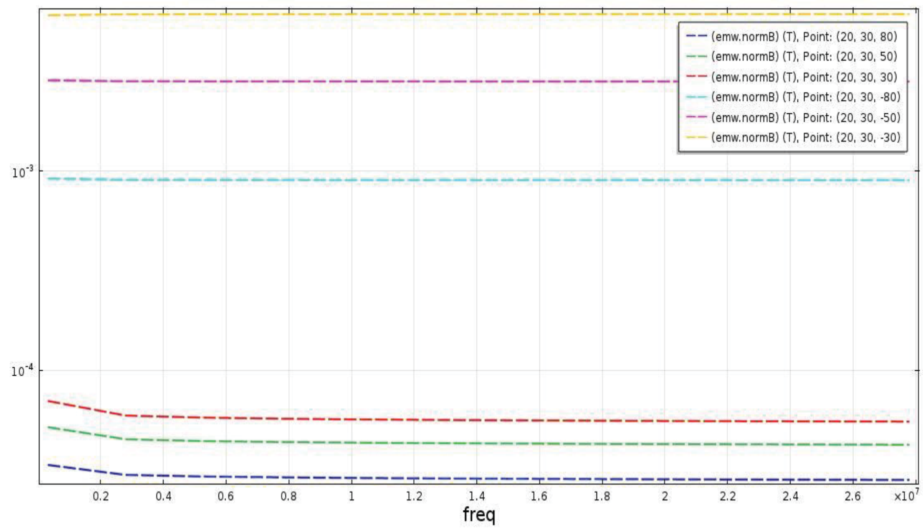

Figure 5. 15. Frequency (Hz) vs Magnetic Flux density for geometry without fillets.

Magnetic flux density for the frequency range shown in table 5.4 flows for both geometries original and modified are showed in Figure 5.14 and Figure 5.15 respectively for fined mesh with target length of 3mm. The behaviour of Magnetic flux density distribution across different cut points 3D looks similar in both geometries.

After comparing the results, the most satisfactory results come from 3mm meshed geometries as compared with others. At cut point 3D (20, 30, 30), flow of magnetic flux density is almost similar for both geometries. The margin of error in accuracy between both geometries is around 0.493%. While at other point (20, 30, 50) error percentage is less around 3.05%. Other points take error percentage up to 6.5% on average. The analysis shows similar behaviour for both geometries with acceptable percentage of error.

For dense mesh with 3mm target length, simulation time is 36.49% less for modified geometry as compared to geometry with fillets. While memory consumption is 39.54% more in geometry with fillets as compared to other one.

While for 15mm target length and 6mm target length for both geometries, the percentage of error in accuracy is very high. Error of margin is up to 90%

to 60% respectively. Due to higher margin of error with coarse mesh, dense mesh with 3mm target length is suitable for desired results after analysis. As the percentage of error is less than 5% for refine mesh. The denser mesh has been applied of different discretization length on geometries, but system crashes during computing analysis due to the limitations of the simulating computer.

Fillets in geometries can be removed to save computational time and memory consumption. As geometry is meshed suitably, margin of error has been reduced up to 5%. Simulation time and memory consumption is reduced more than 36% and nearly 40%respectively.

The quality of the mesh is determined by the shape of individual cells. If the quality of one cell is poor, it can cause inaccurate result or convergence. Meshing around fillets cause distorted cells, due to that computing time and memory consumption increases. Complex CAD geometries like passenger car can be simplified to reduce computational time and memory consumption by removing fillets.

5.3 CAD Geometry with Hole of 20 mm Diameter

The CAD geometries in Figure 5.16 are in ANSA. Original CAD model has hole of 20mm diameter. The hole is removed to get smooth surface on the other geometry.

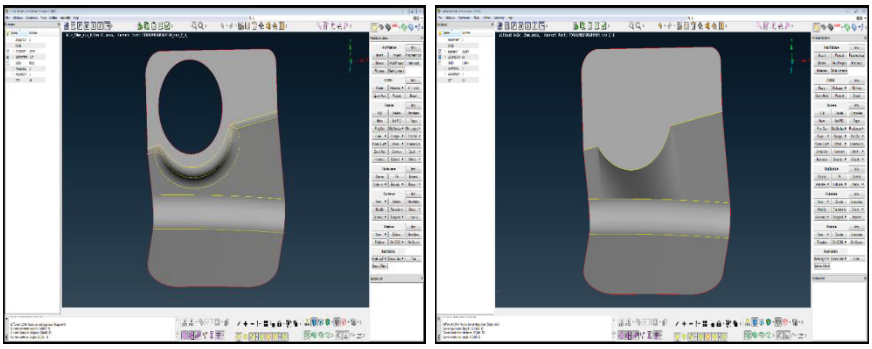

Figure 5. 16. CAD geometry with and without hole.

The finite element mesh is generated on the both models with different discretization lengths. The Target length of mesh varies from 3mm and 1mm. After generating mesh in ANSA, The CAD files are exported as Nastran from ANSA. Nastran files are converted into STL files. STL files are opened in COMSOL. RF module with electromagnetic waves is applied in COMSOL.

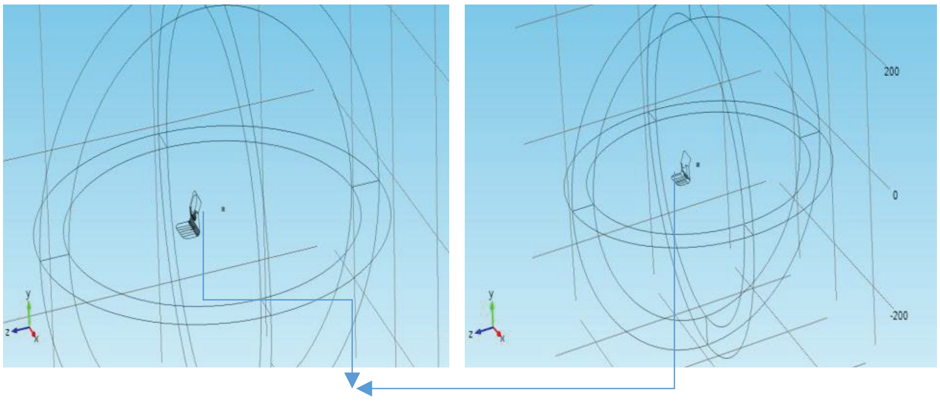

Figure 5. 17. Magnetic dipole moment on geometries with hole and without hole.

The magnetic point dipole is fixed on both geometries as shown in Figure 5.17. The analysis is performed in COMSOL for both geometries with and without hole up to five different cut points of 0mm, 40mm, and 80mm for x, y, z coordinates respectively.

Table 5.5: Solution details of both CAD geometries with 1mm target length.

Original CAD Geometry with hole	**CAD Geometry without hole**
Tetrahedral elements: 41704	Tetrahedral elements: 20675
Triangular elements: 4486	Triangular elements: 2268
No. of DOF solved for: 280194	No. of DOF solved for: 136028
Solution time: 7126 s	Solution time: 1295 s

Physical memory: 5427 MB	Physical memory: 2452 MB

All geometries were analysed from coarse to dense mesh. The details of number of elements and number of degrees of freedom for all geometries are given in Table 5.5. Simulation time and memory consumption for original and modified geometries are also mentioned in table for dense mesh of 1mm target length.

The frequency range for analysis of geometry with 20mm diameter hole is given in Table 5.6. Parameter frequency is 3e5 Hz during analysis.

Table 5.6: Frequency (Hz) range used for analysis of 20mm diameter hole.

Frequency (Hz)
3e5
2.8e6
5.3e6
7.8e6
1.03e7
1.28e7
1.53e7
1.78e7
2.03e7
2.28e7
2.53e7
2.78e7

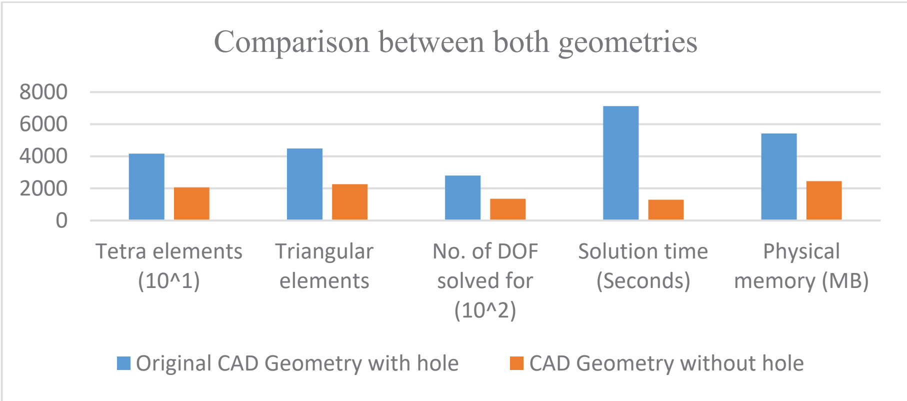

Figure 5. 18. Difference between variables for 20mm diameter hole.

The Figure 5.18 shows, bars are quite high for geometry with hole of 20mm as compared to geometry without hole. Tetrahedral elements are more than 50% in geometry with hole, while triangular elements are nearly 50% more in geometry with hole. Therefore, simulation time and memory consumption show large difference for both geometries. Simulation time is almost 82% more in original geometry while memory consumption is high around 55% in original geometry.

The analysis was performed on five different cut points for both geometries. The percentage of error was at most 17.6% at cut point (0, 15, -10) while on other cut points the percentage of error fluctuated between 30% and 40%. This is quite a high ratio of accuracy loss considering the threshold accuracy error is 5%. If holes with 20mm diameter or bigger than 20mm diameter are removed from CAD geometry, accuracy loss would exceed the acceptable margin. Therefore, larger holes cannot be removed from complex CAD geometries.

If 82% of simulation time and 55% of memory consumption are reduced by losing accuracy of 17.6% in results, decision depends clearly upon CAE simulating engineer. Either strictly want to follow the acceptable loss under 5% or can compromise with loss of accuracy more than 5% to reduce huge percentage of simulation time.

5.4 CAD Geometry with Holes of up to 12 mm Diameter

The CAD geometries with holes and smooth surface are in ANSA as Figure 5.19. Original CAD model is with fourteen holes under 12mm diameter. In which nine holes are 10mm to 12mm diameters. While one hole belongs to 2mm diameter and remaining holes belong up to 4mm diameters. All holes are removed to get smooth surface for analysis purpose.

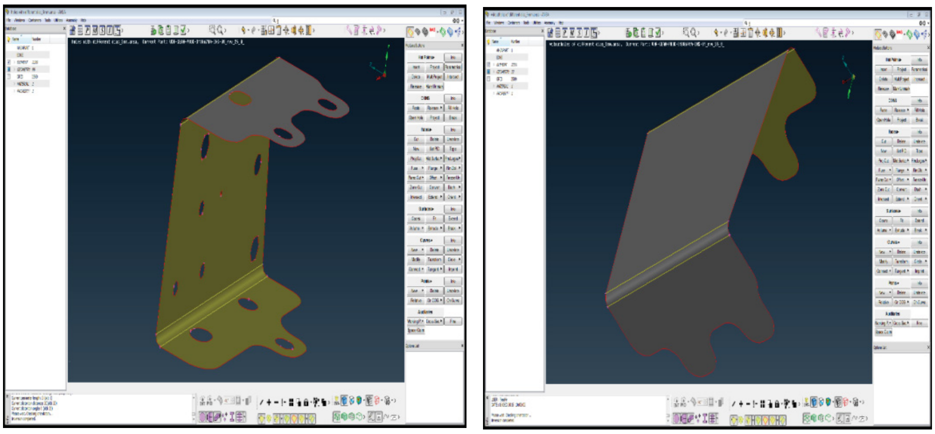

Figure 5. 19. CAD geometries with holes of different diameters and smooth surface respectively.

The finite element mesh is generated on the both models with different discretization lengths. The Target length of mesh varies from 10mm, 6mm and 3mm. After meshing in ANSA, both geometries are exported as Nastran files from ANSA. Nastran files are converted into STL files.

The STL files are exported into COMSOL where the magnetic dipole moment is applied as shown in Figure 5.22 for both geometries.

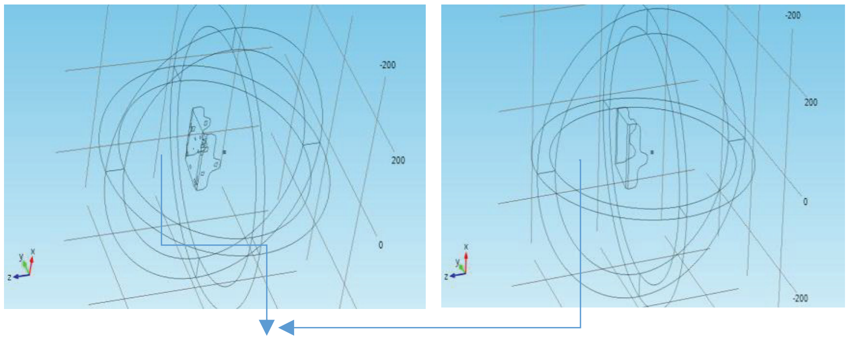

Figure 5. 20. Magnetic dipole moment on geometries with holes and without holes.

The cut points vary for each discretization length. Three different target lengths were used to analyse both geometries. For 10mm target length, analysis was performed on nine different locations, while for 6mm target length, eight cut points were applied and for last target length of 3mm, only two cut points were used. Different target lengths were used to get the idea for suitable mesh in terms of accuracy. Therefore, from coarse to dense mesh, the percentage of error in accuracy and computing time and memory consumption were analysed.

Frequency is constant for all discretization lengths during analysis. Frequency range is displayed in Table 5.7. Parameter frequency is 3e5 Hz during analysis.

Table 5.7. Frequency (Hz) range used for analysis of geometries with and without holes of different diameters.

Frequency (Hz)
3e5
2.8e6
5.3e6
7.8e6

Frequency (Hz)
1.03e7
1.28e7
1.53e7
1.78e7
2.03e7
2.28e7
2.53e7
2.78e7

5.4.1 Analysis for 10mm discretization length

Table 5.8. *Meshing and Solution details of both geometries for 10mm target length.*

CAD Geometry with holes of different diameters	**Modified CAD Geometry without holes**
Tetrahedral elements: 14611	Tetrahedral elements: 12396
Triangular elements: 2134	Triangular elements: 1932
No. of DOF solved for: 96852	No. of DOF solved for: 81858
Solution time: 614 s	Solution time: 420 s
Physical memory: 1786 MB	Physical memory: 1504 MB

Results after meshing with target length of 10mm and analysis for both geometries are presented in Table 5.8. Results have been drawn in figure 5.21. Red bars represent original CAD geometry with 14 holes. Red bars are high for all variables. After meshing, number of elements and degrees of freedom need to be solved for are higher in geometry with holes as compared to modified geometry. Computing time and memory consumption bars are also higher in figure 5.21 for original CAD geometry.

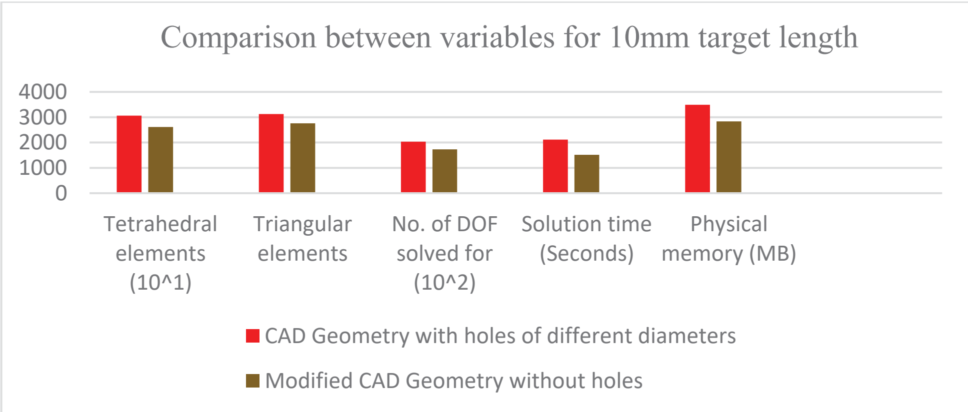

Figure 5. 21. Difference between variables for both geometries for 10mm target length.

For 10mm discretization length, nine cut points 3D was used to analyse the behaviour of magnetic flux density distribution across the both geometries. These cut points cover the whole geometry for analysis from top to bottom. At cut point (40, 10,100) minimum percentage of error in accuracy is around 0.08% while maximum percentage of error is 1.11% which is satisfactory result. On the other three cut points (50, -30, 100), (0, 0 100) and (30, 10, 100), the percentage of error in accuracy is varies from 0.75% to 4.11% which falls within the acceptable margin of accuracy. On the remaining cut points, percentage of error was more than 5%. The computing time was 31.5% less in smooth geometry compared to geometry with holes for coarse mesh with target length of 10mm.15.6% more of memory use was noted in geometry with holes.

The satisfactory results were obtained with coarse mesh, but still both geometries were analysed by applying dense mesh. Results for both meshing of target length 6mm and 3mm are presented below. Later results were compared with each other, which helped to use target length on geometries according to the situation.

5.4.2 Analysis for 6mm Discretization Length

After meshing with target length of 6mm and after analysis, results for both geometries are presented in Table 5.9.

Table 5.9. Meshing and solution details for both geometries for 6mm target length.

CAD Geometry with holes of different diameters	**Modified CAD Geometry without holes**
Tetrahedral elements: 20490	Tetrahedral elements: 15354
Triangular elements: 2354	Triangular elements: 2112
No. of DOF solved for: 135150	No. of DOF solved for: 101484
Solution time: 977 seconds	Solution time: 705 seconds
Physical memory: 2350 MB	Physical memory: 1890 MB

The results in Table 5.9 have been drawn in figure 5.22. Mesh is dense than previous target length of 10mm. Therefore, number of elements and degrees of freedom were higher for 6mm target length. Original CAD geometry had red bars for all variables, which a higher comparing with others. Computing time and memory consumption are also higher for geometry with holes.

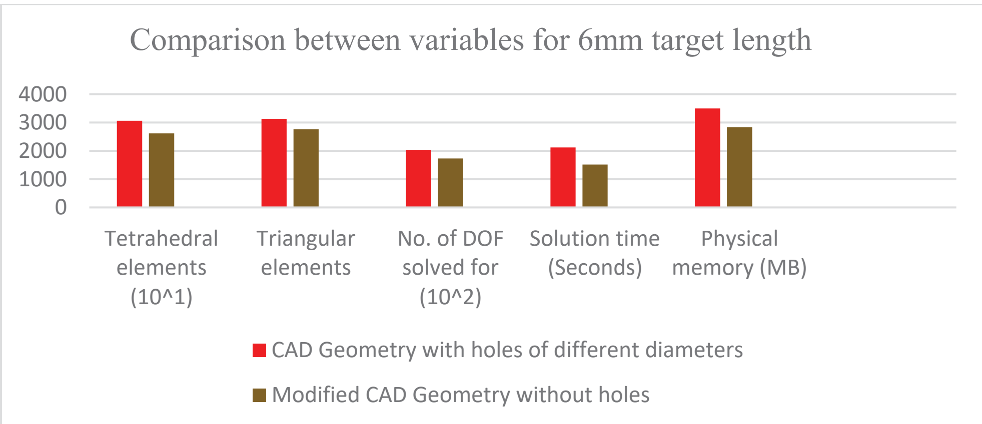

Figure 5. 22. Difference between variables for both geometries for 6mm target length.

Cut points 3D used during analysis for geometries were eight. Magnetic dipole moment shows quite similar behaviour with less percentage of error on three cut points. (40, 10, 100) is cut point where, minimum percentage of error between both geometries is 0.02 percent and maximum percentage of error is 1.478 percent. On the other two cut points (0, 0, 100) and (30, 10, 100) percentage of error is less than 2.4 percent. The other cut points show percentage of error more than 5 percent. Computing time is 27.84 percent less in modified geometry as compared to original geometry. While memory has been consumed 19.5 percent more in original CAD geometry for 6mm target length meshing.

5.4.3 Analysis for 3mm Discretization Length

For the third case, both geometries are same. One is with 14 holes and other geometry is completely smooth. Only difference in this is denser mesh as compared to previous two cases. There are two cut points used to get results for comparing magnetic flux density distribution across both geometries. Meshing and computing details are given in following table.

Table 5.10. Meshing and solution details for both geometries for 3mm target length.

CAD Geometry with holes of different diameters	**Modified CAD Geometry without holes**
Tetrahedral elements: 30621	Tetrahedral elements: 26133
Triangular elements: 3128	Triangular elements: 2759
No. of DOF solved for: 203116	No. of DOF solved for: 172972
Solution time: 2118 seconds	Solution time: 1516 seconds
Physical memory: 3493 MB	Physical memory: 2834 MB

All the details in Table 5.10 are drawn in Figure 5.23. Red bars are higher for all variables, as these red bars represent the geometry with holes. That means original CAD geometry has higher number of elements after meshing and higher number of degrees of freedom need to solved as compared to modified smooth geometry. Therefore, simulation time and memory consumption are higher for original CAD geometry as compared to other one. The percentage of error is almost zero for dense meshed geometries. Computing time has been 28.42% less in modified smooth geometry as compared to original geometry. While memory consumption is 18.86% more in original geometry as compared to modified geometry.

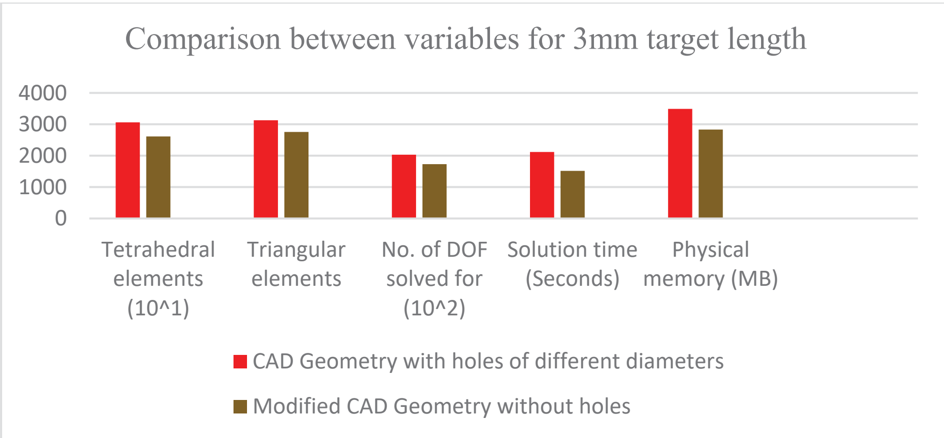

Figure 5. 23. Difference between variables for both geometries for 3mm target length.

Figure 5.24 shows the comparison for simulation time and memory consumption for three meshes used. Coarse mesh is 10mm target length and most dense mesh is with 3mm target length in given scenario. The margin of error for accuracy is acceptable, if it is under 5%. Blue bars represent coarse mesh in figure 5.24. Blue bars are quite low as compared to others. While grey bars represent most dense mesh with 3mm target length. Grey bars are quite high as compared to other bars which mean the simulation time and memory consumption are higher for dense mesh than other meshes. For small CAD geometries, dense mesh can be applied. But for complex CAD models, mesh can be applied from coarse to dense until to get results for acceptable loss of accuracy. For this particular case, 10mm target length is more suitable with acceptable loss of accuracy under 5% and getting reduced simulation time and memory consumption.

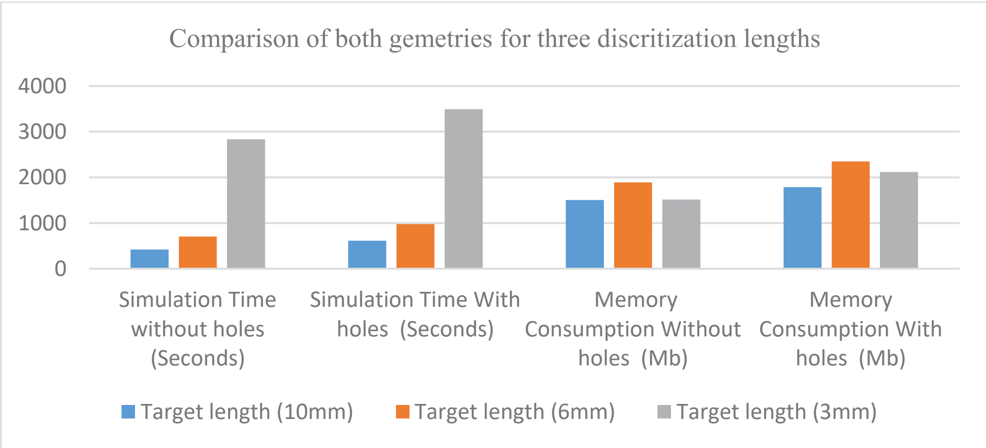

Figure 5. 24. Results comparison from coarse to dense mesh for original and modified geometries.

Holes under or with 12mm diameters can be removed from complex CAD geometries. Simulation time and memory consumption can be reduced nearly 31% and 16% respectively by losing accuracy just under 3%. Complex CAD geometries of passenger car have many small holes which cause convergence. At the result simulation time and physical memory go high. Overall, for bigger parts of CAD geometries, it can be quite relief to do simulations for simulator by filling all holes less than 12mm diameter. Based on the plot presented in *figure 5.24*, it is observable that the simulation times for geometries with holes and without holes (the two main cases explored in the study) exhibit a negative relationship with targeted length. On the other hand, the simulation of memory geometries without holes consumes is slightly lower memory compared to geometries with holes for the three lengths.

6 Discussions

The study employs a combination of strategies to simplify random CAD geometries and validate their CEM simulations. The geometries used in the study were processed on ANSA and exported to COMSOL for simplification and CEM simulations. A comparative analysis of the outcomes is carried out to assess the variations in computational speed and memory consumption of the simulation process. The simulation performance of the computing platform is gauged for geometries with flanges, fillets, and holes with diameters of up to 12mm. Basically, random CAD Geometries with (Figure 5.1) and without flanges (Figure 5.3) were analyzed in CEM Simulations. Bipolar-field (**B-field [µT]** calculations for three different points on the reference and modified modes established flanges can be removed from complex CAD geometries (which can be car/vehicle CAD geometry) with less than 5% loss of accuracy. The analysis of the results targeted the computation performance (memory use and simulation speed) of the simulator and the PC. Removing flanges from complex CAD geometries had a significant reduction in computational time and memory use of the PC. Generally, removing flanges from the geometries has the potential to enhance system performance – no crashes and the ability to support simulations of complex CAD geometries.

Similarly, the behavioral analysis of magnetic flux density distribution across different cut-off points of CAD geometries with fillets and without fillets shown in Figure 5.10 and Figure 5.11 provided critical information on system performance during the simulation process. In figures 5.14 and 5.15, the magnetic flux density at six cut-off points for different frequencies in CAD geometries with and without fillets exhibit similar behaviors in both the reference and modified models. The simulation of the coarse and refined meshes for the two sets of models indicated fillets can be removed from Complex CAD geometries to avoid long simulation time and system crashes during simulations while maintaining accuracy within the 5% threshold.

The analysis of the simulation of random geometries in figure 5.19 with holes of different diameters (left figure) and smooth surface (right figure) showed the removal of holes reduces simulation time and memory use. Variations in the behavior of the magnetic flux density distribution around the holes and the smooth surface were crucial in interpreting the results. The simulation of holes with a diameter of 12mm and below had lower accuracy loss compared to holes with diameters above 12mm. Nonetheless, the overall accuracy loss for all holes fell below the 5% threshold. This demonstrated that removing holes of all diameters from Complex CAD geometries has the potential to reduce computational time and memory use. The CEM simulation of CAD geometries provide a fast and cost-effective method for simplifying and analyzing geometries of different shapes, sizes, and complexities. However, the simulations rely on proprietary software which may not be readily available to all users.

6.1 Strengths and weaknesses

CAD software allows design functionality in 2D as well as 3D workspaces. There are many advantages of using computerized CAD systems. The abundance of features allows a designer to build and design a wide variety of models. The highly technical nature of CAR systems means that the model created using the system can confirm to highly precise standards that industrial projects demand.

However, the upsides also come with some downsides. The wide variety of features and the technical nature of CAD software mean that one will not be able to simply open the software and start creating models. Using CAD-based systems to model parts requires plenty of preparation, skill-building, and money.

High precision and low tolerance make sure that the margin of error for various CAD-created models is also low. This low margin of error is particularly desirable when multiple sub-assemblies have to be fitted together. With CAD, a user can iterate and update the design as many times as needed to get the assemblies to work out. And, there is no money wasted in making expensive prototypes. The only money spent is on the additional time that it takes a designer to make the modifications. If some of your sub-assemblies use different materials, then CAD can give you a clearer idea of how those sub-assemblies with multiple material choices will come together. CAD software has the capability of simulating how different materials will interact with one another.

If one has to do such analysis and simulation in a traditional drafting setup, then it would take much longer.

If some of your sub-assemblies use different materials, then CAD can give you a clearer idea of how those sub-assemblies with multiple material choices will come together. CAD software has the capability of simulating how different materials will interact with one another.

7 Conclusion and Future Work

7.1 Conclusion

The computational electromagnetic (CEM) performed in this study demonstrates that complex CAD models can be simplified by extracting specific details from their geometries with acceptable loss of accuracy, low memory consumption, and minimal computing time. Six relatively small and randomly selected CAD geometries were processed using COMSOL Multiphysics installed in a PC with 8.0 GB RAM, AMD A6-5350M APU with Radeon(tm) HD Graphics 2.90GHz Processer, and 64-bit operation system. The CEM simulations of CAD geometries with flanges, fillets, and holes of different diameter facilitated the identification of the CAD entities liable for removal to simplify the models. These CAD details cause very dense mesh and results in very higher simulation time and memory consumptions. A good trade-off between accuracy, computing time, and memory consumption was achieved by various simplifications of small features in CAD geometries. The EMC analysis of removed flanges, fillets, and holes of up to 12mm diameter noted there was limited effect on the accuracy of the models. A 12 mm was possible to use and gain less computational effort without compromising the measured electromagnetic properties. Hole with 20mm diameter has been analysed in this study by applying EMC simulation. Around 82% simulation time has been reduced and 55% memory consumption has been reduced. The percentage of error in accuracy is 17.6%, which is higher than 5% margin of error. This is quite a big difference between simulation time and memory consumption for geometry with hole of 20mm diameter. Recommendation is to analyse EMC simulations for 20mm diameter holes and holes with higher diameters than 20mm for the studied types of applications.

Similarly, the memory consumption and computational time were reduced drastically. A comparative analysis of EMC simulations of flanges and fillets removal in reference and modified geometries indicated there were at least 70% and 35% reduction in computational time respectively. The usage of the PC memory reduced by 37% and 39% for reference and modified geometries respectively. The overall accuracy of the models was reduced by 2%. The elimination of holes with a diameter of 12mm or below from the geometries was achieved with accuracy errors of zero and 4% for dense mesh and coarse mesh respectively. The computation time for the coarse mesh reduced to 31%

while the memory consumption was capped at 16%. On the other hand, the computation time for the refined mesh was reduced below 28% with memory usage floating at 19%.

This thesis has addressed issues related to the automated detection and elimination, using local mesh modification tools, of poor-quality mesh entities resulting from the presence of geometric model features smaller than the local mesh size required to maintain optimal solution convergence rates. Validity of the locally modified mesh, concerning the original geometric model, is ensured by using the concept of multiple mesh entity classification and defining local topology based constraints to prevent dimensional reduction in the mesh model, The implementation of the presented procedure within the Finite Octree mesh generator [1] resulted in order(s) of magnitude improvement in the mesh quality in terms of worst aspect ratio and smallest dihedral angle metrics for geometric models with small features. The overhead, on the total mesh time, of including the procedure presented in this thesis, has been minimal.

The results of the CEM simulations in the case study demonstrates that complex CAD geometries can be simplified with minimal computation resources without compromising their accuracy. The excision of entities including holes, fillets, and flanges adds value system performance by reducing computational requirements. Savings made on memory consumption alleviates possible system failure/crash which guarantees the simulations of complex CAD geometries at high speed.

7.2 Future Work

The outcomes of the study provide valuable information on optimal methods for simplifying CAD geometries by eliminating holes, fillets, and flanges. However, the study simulated simple CAD geometries due to limitations of computational power. Future studies should perform EMC analysis on complex geometries using powerful computer systems to confirm and/or disapprove results obtained in the current study. The frequency range during EMC analysis is up to 30 MHz for geometries analysed in COMSOL. Higher Frequency ranges can be used for future analysis.

Future works should check importance of information lost by saving more than 80% computing time and 55% memory consumption. Furthermore, this found threshold should be widely applicable for the studied types of applications since it had been proven by other scholars in the literature review.

8 References

[1] C. Li, S. Fan, and M. Shi, “Preparation of CAD model for finite element analysis,” in *2010 International Conference on Computer, Mechatronics, Control and Electronic Engineering (CMCE)*, 2010, vol. 2, pp. 491–494.

[2] D. Krutilek and Z. Raida, “Optimal meshing for high-frequency analysis of realistic structure,” in *2015 Conference on Microwave Techniques (COMITE)*, 2015, pp. 1–4.

[3] M. W. Beall, J. Walsh, and M. S. Shephard, “Accessing CAD Geometry for Mesh Generation.,” in *IMR*, 2003, pp. 33–42.

[4] G. Butlin and C. Stops, “CAD data repair,” in *Proceedings of the 5th International Meshing Roundtable*, 1996, pp. 7–12.

[5] A. A. Mezentsev and T. Woehler, “Methods and Algorithms of Automated CAD Repair for Incremental Surface Meshing.,” in *IMR*, 1999, pp. 299–309.

[6] S. Dey, M. S. Shephard, and M. K. Georges, “Elimination of the adverse effects of small model features by the local modification of automatically generated meshes,” *Eng. Comput.*, vol. 13, no. 3, pp. 134–152, 1997.

[7] M. S. Shephard, M. W. Beall, and R. M. O’Bara, “Revisiting the Elimination of the Adverse Effects of Small Model Features in Automatically Generated Meshes.,” in *IMR*, 1998, pp. 119–131.

[8] R. Sun, S. Gao, and W. Zhao, “An approach to B-rep model simplification based on region suppression,” *Comput. Graph.*, vol. 34, no. 5, pp. 556–564, Oct. 2010.

[9] S. Gao, W. Zhao, H. Lin, F. Yang, and X. Chen, “Feature suppression based CAD mesh model simplification,” *Comput.-Aided Des.*, vol. 42, no. 12, pp. 1178–1188, Dec. 2010.

[10]G. Foucault, J.-C. Cuillière, V. François, J.-C. Léon, and R. Maranzana, “Adaptation of CAD model topology for finite element analysis,” *Comput.-Aided Des.*, vol. 40, no. 2, pp. 176–196, Feb. 2008.

[11]A. Thakur, A. G. Banerjee, and S. K. Gupta, “A survey of CAD model simplification techniques for physics-based simulation applications,” *Comput.-Aided Des.*, vol. 41, no. 2, pp. 65–80, Feb. 2009.

[12]A. Sheffer, “Model simplification for meshing using face clustering,” *Comput.-Aided Des.*, vol. 33, no. 13, pp. 925–934, Nov. 2001.

[13] K. Inoue, T. Itoh, A. Yamada, T. Furuhata, and K. Shimada, “Face clustering of a large-scale CAD model for surface mesh

generation," *Comput.-Aided Des.*, vol. 33, no. 3, pp. 251–261, Mar. 2001.
[14]H. Zhu and C. H. Menq, "B-Rep model simplification by automatic fillet/round suppressing for efficient automatic feature recognition," *Comput.-Aided Des.*, vol. 34, no. 2, pp. 109–123, Feb. 2002.
[15]S. Venkataraman, M. Sohoni, and R. Rajadhyaksha, "Removal of Blends from Boundary Representation Models," in *Proceedings of the Seventh ACM Symposium on Solid Modeling and Applications*, New York, NY, USA, 2002, pp. 83–94.
[16]A. Nogueira de Sao Jose, A. C. P. M. Colin, J. Fujioka Mologni, G. Maciulis Dip, U. do Carmo Resende, and S. Trindade Mordente Goncalves, "Computational savings based on Three-Dimensional automotive geometries' simplifications in electromagnetics simulations," in *Microwave Optoelectronics Conference (IMOC), 2013 SBMO/IEEE MTT-S International*, 2013, pp. 1–5.
[17]S. B. Andersen, I. F. Santos, and A. Fuerst, "Investigation of Model Simplification and Its Influence on the Accuracy in FEM Magnetic Calculations of Gearless Drives," *IEEE Trans. Magn.*, vol. 48, no. 7, pp. 2166–2177, Jul. 2012.
[18]S. Savia, R. Langley, and A. Walbeoff, "Automotive Antenna Simulation," in *The Second European Conference on Antennas and Propagation, 2007. EuCAP 2007*, 2007, pp. 1–4.
[19]S. Frei, R. G. Jobava, and D. Topchishvili, "Complex approaches for the calculation of EMC problems of large systems," in *2004 InternationalSymposium on Electromagnetic Compatibility, 2004. EMC 2004*, 2004, vol. 3, pp. 826–831 vol.3.
[20]J. A. Flint and A. R. Ruddle, "The GEMCAR project–generic guidelines for the modelling of automotive EMC," in *Proceedings of ARMMS 2001 RF and Microwave Conference*, 2001.
[21]A. R. Ruddle, "THE EU FRAMEWORK V PROJECT 'GEMCAR': PRACTICAL ASPECTS OF THE DEVELOPMENT OF WHOLE VEHICLE ELECTROMAGNETIC MODELS."
[22]"ansa_v15.0.x_users_guide.pdf." .

8 Appendix

Appendix 1

The following properties are constant for all the CAD geometries, which are analysed in COMSOL.

Materials

Material one (Steel)

Name	Value	Unit
Relative permeability	200	1
Relative permittivity	1	1
Electrical conductivity	1E7	S/m

Table 1.1: Material one (Steel) parameters.

Description	Value
Electrical conductivity	{{1e7, 0, 0}, {0, 1e7, 0}, {0, 0, 1e7}}
Relative permittivity	{{1, 0, 0}, {0, 1, 0}, {0, 0, 1}}
Relative permeability	{{200, 0, 0}, {0, 200, 0}, {0, 0, 200}}

Table1.2: Basic Settings for material one.

Material two (Air)

Name	Value	Unit
Electrical conductivity	0	S/m
Relative permittivity	1	1
Relative permeability	1	1

Table 1.3: Material two (Air) parameters.

Description	Value
Electrical conductivity	{{0, 0, 0}, {0, 0, 0}, {0, 0, 0}}
Relative permittivity	{{1, 0, 0}, {0, 1, 0}, {0, 0, 1}}
Relative permeability	{{1, 0, 0}, {0, 1, 0}, {0, 0, 1}}

Table 1.4: Basic Settings for material two.

Physics used in COMSOL for CAD geometries is Electromagnetic waves, Frequency domain (emw). Where Frequencies range (300000, 5000000, 30000000) in Hz.

Name	Value
Expression	emw.normB
Unit	T
Description	Magnetic flux density norm

Table 1.5: Expression for magnetic flux density norm

Appendix 2

It consists of magnetic flux density norm on different cut points 3D in tables form for geometries with fillets and without fillets. Both geometries are analysed for three different discretization lengths of 3mm, 6mm and 15mm, Magnetic flux density norm is presented in tables for both geometries with each discretization length respectively.

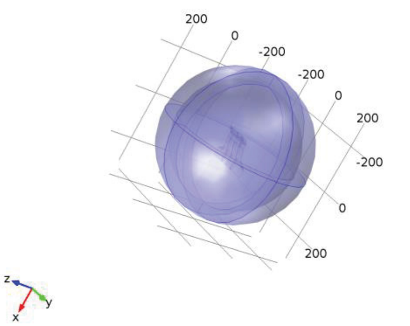

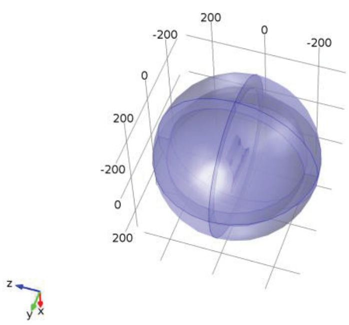

Figure 2.1: Perfectly matched layer for Electromagnetic Waves, Frequency Domain for geometries with and without fillets.

Table 2.1: Magnetic flux density norm for CAD geometry with fillets for 3mm target length at different cut points 3D.

Frequency (Hz)	Magnetic flux density norm (T), Point: (20, 30, 80)	Magnetic flux density norm (T), Point: (20, 30, 50)	Magnetic flux density norm (T), Point: (20, 30, 30)	Magnetic flux density norm (T), Point: (20, 30, -80)	Magnetic flux density norm (T), Point: (20, 30, -50)	Magnetic flux density norm (T), Point: (20, 30, -30)
3e5	2.87553e5	4.82282e5	6.68303e5	8.49153e4	0.00305	0.00494
5.3e6	2.57726e5	4.21622e5	5.68875e5	8.39292e4	0.00303	0.005
1.03e7	2.54725e5	4.15488e5	5.59023e5	8.38414e4	0.00303	0.005
1.53e7	2.53332e5	4.12577e5	5.54286e5	8.38041e4	0.00303	0.005
2.03e7	2.52531e5	4.10841e5	5.51414e5	8.37848e4	0.00303	0.005
2.53e7	2.52042e5	4.09713e5	5.49498e5	8.37751e4	0.00302	0.005

Table 2.2: Magnetic flux density norm for CAD geometry without fillets for 3mm target length at different cut points 3D.

Frequency (Hz)	**(emw.normB) (T), Point: (20, 30, 80)**	**(emw.normB) (T), Point: (20, 30, 50)**	**(emw.normB) (T), Point: (20, 30, 30)**	**(emw.normB) (T), Point: (20, 30, -80)**	**(emw.normB) (T), Point: (20, 30, -50)**	**(emw.normB) (T), Point: (20, 30, -30)**
3e5	3.33903 e5	5.16762 e5	7.00005 e5	9.1437e 4	0.00286	0.00606
2.8e6	2.97343 e5	4.49015 e5	5.90562 e5	9.03755 e4	0.00283	0.00613
5.3e6	2.92047 e5	4.39864 e5	5.76881 e5	9.02392 e4	0.00282	0.00613
7.8e6	2.89108 e5	4.34938 e5	5.69665 e5	9.017e4	0.00282	0.00614
1.03e7	2.87013 e5	4.31553 e5	5.6483e 5	9.01232 e4	0.00282	0.00614
1.28e7	2.85528 e5	4.29198 e5	5.61434 e5	9.00895 e4	0.00282	0.00614
1.53e7	2.84363 e5	4.27388 e5	5.58833 e5	9.00632 e4	0.00282	0.00614
1.78e7	2.83382 e5	4.25891 e5	5.56719 e5	9.00418 e4	0.00282	0.00614
2.03e7	2.82539 e5	4.24626 e5	5.54961 e5	9.00241 e4	0.00282	0.00614
2.28e7	2.81807 e5	4.23546 e5	5.53482 e5	9.00095 e4	0.00282	0.00615
2.53e7	2.81166 e5	4.22616 e5	5.52221 e5	8.99973 e4	0.00282	0.00615
2.78e7	2.80601 e5	4.21805 e5	5.51133 e5	8.99871 e4	0.00282	0.00615

Table 2.3: Magnetic flux density norm for CAD geometry with fillets for target length of 6mm at two cut points 3D.

Frequency (Hz)	Magnetic flux density norm (T), Point: (0, 0, 80)	Magnetic flux density norm (T), Point: (0, 0, 50)
3e5	1.54284e4	3.89249e4
2.8e6	1.54109e4	3.89067e4
5.3e6	1.5394e4	3.8889e4
7.8e6	1.53777e4	3.88721e4
1.03e7	1.5362e4	3.8856e4
1.28e7	1.53471e4	3.88408e4
1.53e7	1.5333e4	3.88266e4
1.78e7	1.53198e4	3.88134e4
2.03e7	1.53075e4	3.88014e4
2.28e7	1.52961e4	3.87905e4
2.53e7	1.52856e4	3.87808e4
2.78e7	1.52762e4	3.87723e4

Table 2.4: Magnetic flux density norm for CAD geometry without fillets for target length of 6mm at two cut points 3D.

Frequency (Hz)	Magnetic flux density norm (T), Point: (0, 0, 80)	Magnetic flux density norm (T), Point: (0, 0, 50)
3e5	1.54284e4	3.89249e4
2.8e6	1.54109e4	3.89067e4
5.3e6	1.5394e4	3.8889e4
7.8e6	1.53777e4	3.88721e4
1.03e7	1.5362e4	3.8856e4
1.28e7	1.53471e4	3.88408e4
1.53e7	1.5333e4	3.88266e4
1.78e7	1.53198e4	3.88134e4
2.03e7	1.53075e4	3.88014e4
2.28e7	1.52961e4	3.87905e4
2.53e7	1.52856e4	3.87808e4
2.78e7	1.52762e4	3.87723e4

Table 2.5: Magnetic flux density norm for CAD geometry with fillets for target length of 15mm at different cut points 3D.

Frequency (Hz)	Magnetic flux density norm (T), Point: (20, 30, 80)	Magnetic flux density norm (T), Point: (20, 30, 50)	Magnetic flux density norm (T), Point: (20, 30, 30)	Magnetic flux density norm (T), Point: (20, 30, -80)	Magnetic flux density norm (T), Point: (20, 30, -50)	Magnetic flux density norm (T), Point: (20, 30, -30)
3e5	3.28289e5	5.04409e5	6.65322e5	4.22537e4	0.00344	0.0068
2.8e6	2.96529e5	4.46633e5	5.76928e5	4.18377e4	0.00343	0.00685
5.3e6	2.91117e5	4.37091e5	5.62604e5	4.17678e4	0.00342	0.00686
7.8e6	2.88292e5	4.32262e5	5.5547e5	4.17276e4	0.00342	0.00686
1.03e7	2.86367e5	4.29055e5	5.50776e5	4.1706e4	0.00342	0.00686
1.28e7	2.84907e5	4.26705e5	5.47404e5	4.16906e4	0.00342	0.00686
1.53e7	2.83733e5	4.24873e5	5.44817e5	4.16783e4	0.00342	0.00686
1.78e7	2.82755e5	4.23391e5	5.42758e5	4.16682e4	0.00342	0.00686
2.03e7	2.81922e5	4.22161e5	5.41074e5	4.16598e4	0.00342	0.00686
2.28e7	2.81201e5	4.21121e5	5.3967e5	4.16527e4	0.00342	0.00687
2.53e7	2.80573e5	4.20232e5	5.38481e5	4.16469e4	0.00342	0.00687
2.78e7	2.80022e5	4.19466e5	5.37467e5	4.16422e4	0.00342	0.00687

Table 2.6: Magnetic flux density norm for CAD geometry without fillets for target length of 15mm at different cut points 3D.

Frequency (Hz)	Magnetic flux density norm (T), Point: (20, 30, 80)	Magnetic flux density norm (T), Point: (20, 30, 50)	Magnetic flux density norm (T), Point: (20, 30, 30)	Magnetic flux density norm (T), Point: (20, 30, -80)	Magnetic flux density norm (T), Point: (20, 30, -50)	Magnetic flux density norm (T), Point: (20, 30, -30)
3e5	6.15317e5	8.33974e5	0.00322	3.49407e4	0.00112	0.0026
2.8e6	5.43424e5	6.87162e5	0.00322	3.47225e4	0.00112	0.0026
5.3e6	5.31573e5	6.98806e5	0.00322	3.46774e4	0.00112	0.0026
7.8e6	5.25349e5	7.00271e5	0.00322	3.46478e4	0.00112	0.0026
1.03e7	5.20856e5	6.97062e5	0.00322	3.46243e4	0.00112	0.0026
1.28e7	5.1653e5	6.91586e5	0.00322	3.46036e4	0.00112	0.0026
1.53e7	5.13363e5	6.85351e5	0.00322	3.45858e4	0.00112	0.0026
1.78e7	5.11344e5	6.79876e5	0.00322	3.45705e4	0.00112	0.0026
2.03e7	5.0984e5	6.75853e5	0.00322	3.4557e4	0.00112	0.0026
2.28e7	5.08602e5	6.73107e5	0.00322	3.45449e4	0.00112	0.0026
2.53e7	5.07547e5	6.71171e5	0.00322	3.45342e4	0.00112	0.0026
2.78e7	5.06636e5	6.69719e5	0.00322	3.45248e4	0.00112	0.0026

Appendix 3

It consists of magnetic flux density norm on different cut points 3D in table forms for geometries with hole of 20mm diameter and without hole. Magnetic flux density norm is presented for discretization length of 1mm.

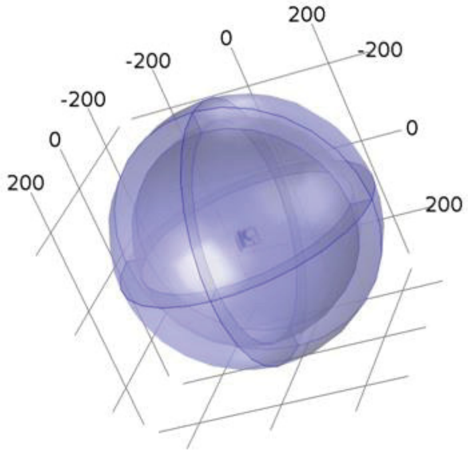

Figure3.1: Perfectly matched layer for Electromagnetic Waves, Frequency Domain for geometry with hole of 20mm diameter.

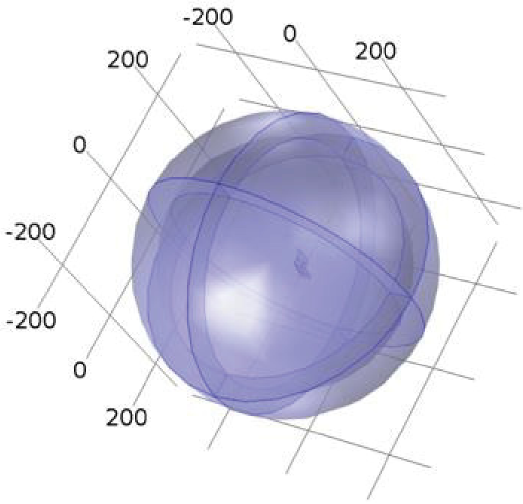

Figure3.2: Perfectly matched layer for Electromagnetic Waves, Frequency Domain for geometry without hole of 20mm diameter.

Table 3.1: Magnetic flux density norm for CAD geometry with hole of 20mm diameter for target length of 1mm at different cut points 3D.

Frequency (Hz)	Magnetic flux density norm (T), Point: (0, 40, 80)	Magnetic flux density norm (T), Point: (0, 30, 60)	Magnetic flux density norm (T), Point: (0, 0, -30)	Magnetic flux density norm (T), Point: (0, 15, -10)	Magnetic flux density norm (T), Point: (20, 20, 70)
3e5	1.55707e4	2.85534e4	0.06078	0.2019	2.20326e4
2.8e6	1.48443e4	2.63635e4	0.06077	0.20188	2.07127e4
5.3e6	1.47161e4	2.60048e4	0.06077	0.20188	2.04925e4
7.8e6	1.46448e4	2.58186e4	0.06077	0.20187	2.03764e4
1.03e7	1.45942e4	2.56948e4	0.06077	0.20187	2.02976e4
1.28e7	1.45545e4	2.56029e4	0.06077	0.20187	2.02378e4
1.53e7	1.45214e4	2.55298e4	0.06077	0.20187	2.01894e4
1.78e7	1.44929e4	2.54693e4	0.06077	0.20187	2.01488e4
2.03e7	1.44679e4	2.54182e4	0.06077	0.20187	2.01139e4
2.28e7	1.44459e4	2.53741e4	0.06077	0.20187	2.00835e4
2.53e7	1.44262e4	2.53357e4	0.06077	0.20187	2.00569e4
2.78e7	1.44087e4	2.53021e4	0.06077	0.20187	2.00334e4

Table 3.2: Magnetic flux density norm for CAD geometry without hole of 20mm diameter for target length of 1mm at different cut points 3D.

Frequency (Hz)	Magnetic flux density norm (T), Point: (0, 40, 80)	Magnetic flux density norm (T), Point: (0, 30, 60)	Magnetic flux density norm (T), Point: (0, 0, -30)	Magnetic flux density norm (T), Point: (0, 15, -10)	Magnetic flux density norm (T), Point: (20, 20, 70)
3e5	2.34777e4	4.76641e4	0.00788	0.16625	3.57849e4
2.8e6	2.14586e4	4.1583e4	0.00785	0.16617	3.19418e4
5.3e6	2.11515e4	4.0712e4	0.00785	0.16616	3.1409e4
7.8e6	2.09894e4	4.02649e4	0.00785	0.16616	3.1135e4
1.03e7	2.08794e4	3.9969e4	0.00785	0.16615	3.09528e4
1.28e7	2.07971e4	3.97527e4	0.00784	0.16615	3.08181e4
1.53e7	2.07313e4	3.95843e4	0.00784	0.16615	3.07117e4
1.78e7	2.06773e4	3.94493e4	0.00784	0.16615	3.06256e4
2.03e7	2.06316e4	3.93378e4	0.00784	0.16615	3.05541e4
2.28e7	2.05923e4	3.9243e4	0.00784	0.16615	3.04933e4
2.53e7	2.05578e4	3.9161e4	0.00784	0.16614	3.04407e4
2.78e7	2.05274e4	3.90894e4	0.00784	0.16614	3.03946e4

Appendix 4

It consists of magnetic flux density norm on different cut points 3D in table forms for geometries with holes of different diameter and without holes. Magnetic flux density norm is presented for discretization length of 10mm, 6mm and 3mm respectively.

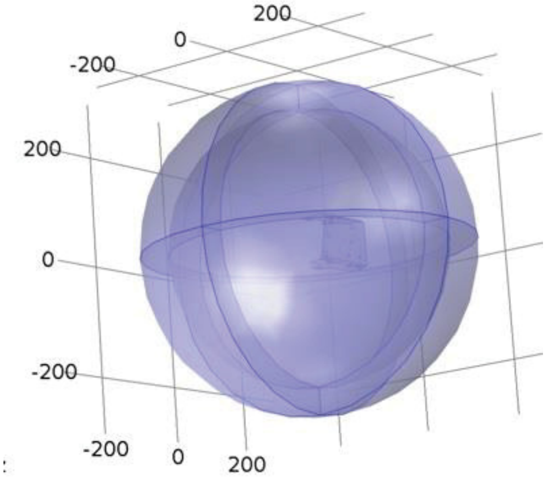

Figure4.1: Perfectly matched layer for Electromagnetic Waves, Frequency Domain for geometry with holes of different diameters.

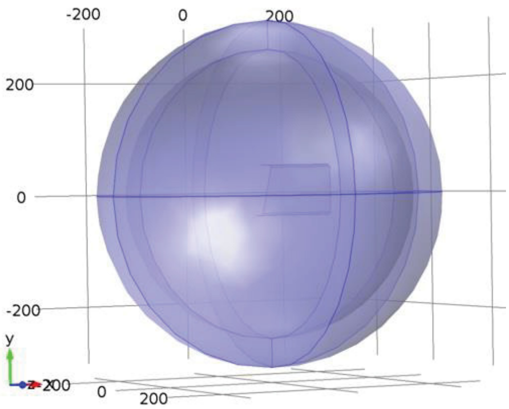

Figure4.2: Perfectly matched layer for Electromagnetic Waves, Frequency Domain for geometry without holes of different diameters.

Table4.1: Magnetic flux density norm for CAD geometry with holes of different diameters for target length of 10mm at different cut points 3D.

Frequency (Hz)	**emw.normB (T), (0, 0, 1.0E2)**	**emw.normB (T), (0, 0, -50)**	**emw.normB (T), (30, 10, 1.0E2)**	**emw.normB (T), (50, -30, 1.0E2)**	**emw.normB (T), (40, 10, 1.0E2)**	**emw.normB (T), (40, 20, -50)**	**emw.normB (T), (40, 10, -20)**	**emw.normB (T), (30, 10, -10)**	**emw.normB (T), (0, 0, -1.0E2)**	**emw.normB (T), (0, 0, -2.0E2)**
3e5	4.11823e5	0.02889	3.00694e5	2.99175e5	2.79498e5	0.00101	0.00271	0.00313	6.13669e4	4.80248e5
2.8e6	3.79017e5	0.02888	2.70781e5	2.72248e5	2.50228e5	0.00101	0.00272	0.00313	6.12225e4	4.70138e5
5.3e6	3.73215e5	0.02888	2.6568e5	2.67379e5	2.4524e5	0.00101	0.00272	0.00313	6.11743e4	4.63245e5
7.8e6	3.70016e5	0.02888	2.62866e5	2.64608e5	2.42475e5	0.00101	0.00272	0.00314	6.11373e4	4.57457e5
1.03e7	3.67756e5	0.02888	2.60878e5	2.62604e5	2.40514e5	0.00101	0.00272	0.00314	6.11055e4	4.52409e5
1.28e7	3.65978e5	0.02888	2.59314e5	2.60995e5	2.38965e5	0.00101	0.00272	0.00314	6.1077e4	4.47911e5
1.53e7	3.645e5	0.02888	2.5801e5	2.59631e5	2.3767e5	0.00101	0.00273	0.00314	6.10512e4	4.43854e5
1.78e7	3.63231e5	0.02888	2.56887e5	2.58439e5	2.3655e5	0.00101	0.00273	0.00314	6.10278e4	4.40167e5

Frequency (Hz)	emw.normB (T), (0, 0, 1.0E2)	emw.normB (T), (0, 0, -50)	emw.normB (T), (30, 10, 1.0E2)	emw.normB (T), (50, -30, 1.0E2)	emw.normB (T), (40, 10, 1.0E2)	emw.normB (T), (40, 20, -50)	emw.normB (T), (40, 10, -20)	emw.normB (T), (30, 10, -10)	emw.normB (T), (0, 0, -1.0E2)	emw.normB (T), (0, 0, -2.0E2)
2.03e7	3.62121e5	0.02888	2.55901e5	2.57378e5	2.35564e5	0.0101	0.0273	0.0314	6.10067e4	4.36803e5
2.28e7	3.61139e5	0.02888	2.55026e5	2.56425e5	2.34685e5	0.0101	0.0273	0.0314	6.09876e4	4.33727e5
2.53e7	3.60266e5	0.02888	2.54243e5	2.55564e5	2.33896e5	0.0101	0.0273	0.0314	6.09706e4	4.30912e5
2.78e7	3.59486e5	0.02888	2.5354e5	2.54782e5	2.33185e5	0.0101	0.0273	0.0314	6.09555e4	4.28335e5

Table4.2: Magnetic flux density norm for CAD geometry without holes of different diameters for target length of 10mm at different cut points 3D.

Frequency (Hz)	emw.normB (T), (0, 0, 1.0 E2)	emw.normB (T), (0, 0, -50)	emw.normB (T), (30, 10, 1.0 E2)	emw.normB (T), (50, -30, 1.0 E2)	emw.normB (T), (40, 10, 1.0 E2)	emw.normB (T), (40, 20, -50)	emw.normB (T), (40, 10, -20)	emw.normB (T), (30, 10, -10)	emw.normB (T), (0, 0, -1.0 E2)	emw.normB (T), (0, 0, -2.0 E2)
3e5	4.03145e5	0.01769	2.8833e5	2.95412e5	2.79725e5	0.00371	0.00217	0.00415	5.3101e4	4.77614e5
2.8e6	3.73114e5	0.01768	2.60955e5	2.69623e5	2.52376e5	0.00371	0.00218	0.00415	5.29605e4	4.67203e5
5.3e6	3.67694e5	0.01768	2.562e5	2.65006e5	2.47619e5	0.00371	0.00218	0.00415	5.29139e4	4.60186e5
7.8e6	3.64611e5	0.01768	2.53531e5	2.62356e5	2.44942e5	0.00371	0.00218	0.00415	5.28782e4	4.54349e5
1.03e7	3.62415e5	0.01768	2.51635e5	2.60432e5	2.43032e5	0.00371	0.00218	0.00415	5.28474e4	4.49289e5
1.28e7	3.60685e5	0.01768	2.50138e5	2.58884e5	2.41516e5	0.00371	0.00218	0.00415	5.28198e4	4.44798e5
1.53e7	3.59244e5	0.01768	2.48888e5	2.57569e5	2.40245e5	0.00371	0.00218	0.00415	5.27949e4	4.40758e5
1.78e7	3.58005e5	0.01768	2.47809e5	2.56418e5	2.39143e5	0.00371	0.00218	0.00415	5.27723e4	4.37093e5

Frequency (Hz)	emw.normB (T), (0, 0, 1.0E2)	emw.normB (T), (0, 0, -50)	emw.normB (T), (30, 10, 1.0E2)	emw.normB (T), (50, -30, 1.0E2)	emw.normB (T), (40, 10, 1.0E2)	emw.normB (T), (40, 20, -50)	emw.normB (T), (40, 10, -20)	emw.normB (T), (30, 10, -10)	emw.normB (T), (0, 0, -1.0E2)	emw.normB (T), (0, 0, -2.0E2)
2.03e7	3.5692e5	0.01768	2.46859e5	2.55391e5	2.3817e5	0.00371	0.00218	0.00415	5.27518e4	4.33754e5
2.28e7	3.55957e5	0.01768	2.46013e5	2.54467e5	2.373e5	0.00371	0.00218	0.00415	5.27333e4	4.30704e5
2.53e7	3.55099e5	0.01768	2.45254e5	2.53629e5	2.36516e5	0.00371	0.00218	0.00415	5.27168e4	4.27915e5
2.78e7	3.54331e5	0.01768	2.44572e5	2.52868e5	2.35809e5	0.00371	0.00218	0.00415	5.27021e4	4.25365e5

Table4.3: Magnetic flux density norm for CAD geometry with holes of different diameters for target length of 6mm at different cut points 3D.

Frequency (Hz)	emw. norm B (T), (0, 0, 1.0E2)	emw. norm B (T), (0, 0, -50)	emw. norm B (T), (30, 10,1. 0E2)	emw. norm B (T), (50, -30,1. 0E2)	emw. norm B (T), (40, 10,1. 0E2)	emw. norm B (T), (40, 20, -50)	emw. norm B (T), (40, 10, -20)	emw. norm B (T), (30, 10, -10)
3e5	4.14838e5	0.02386	2.9767e5	2.96775e5	2.81459e5	0.0018	0.00186	0.00193
2.8e6	3.83349e5	0.02386	2.68018e5	2.70005e5	2.52364e5	0.0018	0.00187	0.00194
5.3e6	3.77744e5	0.02386	2.62986e5	2.65239e5	2.4741e5	0.0018	0.00187	0.00194
7.8e6	3.74607e5	0.02386	2.60203e5	2.62521e5	2.44659e5	0.0018	0.00187	0.00194
1.03e7	3.72385e5	0.02386	2.58242e5	2.60555e5	2.42712e5	0.0018	0.00187	0.00194
1.28e7	3.70639e5	0.02386	2.56702e5	2.58977e5	2.41175e5	0.0018	0.00187	0.00194
1.53e7	3.69188e5	0.02386	2.55421e5	2.57639e5	2.39892e5	0.0018	0.00187	0.00194
1.78e7	3.67941e5	0.02386	2.54319e5	2.56468e5	2.38783e5	0.0018	0.00187	0.00194
2.03e7	3.6685e5	0.02386	2.53352e5	2.55426e5	2.37806e5	0.0018	0.00187	0.00194
2.28e7	3.65883e5	0.02386	2.52492e5	2.54488e5	2.36934e5	0.0018	0.00187	0.00194
2.53e7	3.65022e5	0.02386	2.51723e5	2.53638e5	2.36151e5	0.0018	0.00187	0.00194
2.78e7	3.64252e5	0.02386	2.51031e5	2.52867e5	2.35445e5	0.0018	0.00187	0.00194

Table4.4: Magnetic flux density norm for CAD geometry without holes of different diameters for target length of 6mm at different cut points 3D.

Frequency (Hz)	**emw.norm B (T), (0, 0, 1.0E2)**	**emw.norm B (T), (0, 0, -50)**	**emw.norm B (T), (30,10,1.0E2)**	**emw.norm B (T), (50, -30,1.0E2)**	**emw.norm B (T), (40,10,1.0E2)**	**emw.norm B (T), (40,20, -50)**	**emw.norm B (T), (40,10, -20)**	**emw.norm B (T), (30, 10, -10)**
3e5	4.0975e5	0.01078	2.90291e5	2.97005e5	2.77297e5	0.00137	0.00101	0.0036
2.8e6	3.80649e5	0.01078	2.64079e5	2.72008e5	2.5124e5	0.00136	0.00102	0.00361
5.3e6	3.75383e5	0.01078	2.5956e5	2.67484e5	2.4674e5	0.00136	0.00102	0.00361
7.8e6	3.72407e5	0.01078	2.57025e5	2.64875e5	2.44208e5	0.00136	0.00102	0.00361
1.03e7	3.70284e5	0.01078	2.55216e5	2.62971e5	2.42396e5	0.00137	0.00102	0.00361
1.28e7	3.68606e5	0.01078	2.53783e5	2.61433e5	2.40955e5	0.00137	0.00102	0.00361
1.53e7	3.67206e5	0.01078	2.52582e5	2.60122e5	2.39743e5	0.00137	0.00102	0.00361
1.78e7	3.65999e5	0.01078	2.51543e5	2.58971e5	2.38691e5	0.00137	0.00102	0.00361
2.03e7	3.64939e5	0.01078	2.50627e5	2.57944e5	2.3776e5	0.00137	0.00102	0.00361
2.28e7	3.63999e5	0.01078	2.4981e5	2.57017e5	2.36926e5	0.00137	0.00102	0.00361
2.53e7	3.6316e5	0.01078	2.49077e5	2.56176e5	2.36176e5	0.00137	0.00102	0.00361
2.78e7	3.62409e5	0.01078	2.48416e5	2.55412e5	2.35498e5	0.00137	0.00102	0.00361

Table4.5: Magnetic flux density norm for CAD geometry with holes of different diameters for target length of 3mm at different cut points 3D.

Frequ ency (Hz)	**Magnetic flux density norm (T), Point: (0, 0, 80)**	**Magnetic flux density norm (T), Point: (0, 0, 50)**
3e5	1.54284e4	3.89249e4
2.8e6	1.54109e4	3.89067e4
5.3e6	1.5394e4	3.8889e4
7.8e6	1.53777e4	3.88721e4
1.03e7	1.5362e4	3.8856e4
1.28e7	1.53471e4	3.88408e4
1.53e7	1.5333e4	3.88266e4
1.78e7	1.53198e4	3.88134e4
2.03e7	1.53075e4	3.88014e4
2.28e7	1.52961e4	3.87905e4
2.53e7	1.52856e4	3.87808e4
2.78e7	1.52762e4	3.87723e4

Table4.6: Magnetic flux density norm for CAD geometry without holes of different diameters for target length of 3mm at different cut points 3D.

Frequency (Hz)	**Magnetic flux density norm (T), Point: (0, 0, 80)**	**Magnetic flux density norm (T), Point: (0, 0, 50)**
3e5	1.54284e4	3.89249e4
2.8e6	1.54109e4	3.89067e4
5.3e6	1.5394e4	3.8889e4
7.8e6	1.53777e4	3.88721e4
1.03e7	1.5362e4	3.8856e4
1.28e7	1.53471e4	3.88408e4
1.53e7	1.5333e4	3.88266e4
1.78e7	1.53198e4	3.88134e4
2.03e7	1.53075e4	3.88014e4
2.28e7	1.52961e4	3.87905e4
2.53e7	1.52856e4	3.87808e4
2.78e7	1.52762e4	3.87723e4